

25

26 **Abstract**

27 The ordered assembly of a functional pre-initiation complex (PIC), composed of general
28 transcription factors (GTFs), is a prerequisite for the transcription of protein-coding genes by
29 RNA polymerase II. TFIID, comprised of the TATA binding protein (TBP) and 13 TBP-
30 associated factors (TAFs), is the GTF that is thought to recognize the promoter sequences
31 allowing site-specific PIC assembly. Transcriptional cofactors, such as SAGA, are also
32 necessary for tightly regulated transcription initiation. The contribution of the two TAF10-
33 containing complexes (TFIID, SAGA) to erythropoiesis remains elusive. By ablating TAF10
34 specifically in erythroid cells *in vivo* we observed a differentiation block accompanied by
35 deregulated GATA1 target genes, including *Gata1* itself, suggesting functional crosstalk
36 between GATA1 and TAF10. Additionally, we analyzed the composition of TFIID and SAGA
37 complexes by mass spectrometry in mouse and human cells and found that their global
38 integrity is maintained, with minor changes, during erythroid differentiation and
39 development. In agreement with our functional data, we show that TAF10 interacts directly
40 with GATA1 and that TAF10 is enriched on the GATA1 locus in human fetal erythroid cells.
41 Thus, our findings demonstrate a crosstalk between canonical TFIID and SAGA complexes
42 and cell-specific transcription activators during development and differentiation.

43

44 Introduction

45

46 Initiation of RNA polymerase II (RNA pol II) transcription in eukaryotes is a process
47 involving stepwise recruitment and assembly of the preinitiation complex (PIC) at the core
48 promoter of a transcriptional unit. Transcription factor TFIID, comprised of the TATA binding
49 protein (TBP) and a series of TBP-associated factors (TAFs), is the general transcription
50 factor (GTF) that by recognizing the promoter sequences and surrounding chromatin marks,
51 allows the site-specific assembly of the PIC(1) (and refs therein). Binding of the TFIID
52 complex is aided by TFIIA and followed by the remainder of the general transcription
53 machinery, including TFIIB, RNA pol II/TFIIF, TFIIE and TFIIH complexes. Additional
54 cofactors, including the Mediator complex, histone modifiers and chromatin remodelers,
55 facilitate the communication between gene-specific transcription factors and the general
56 transcription machinery.

57 The TFIID complex does not only bind to TATA box-containing promoters, but also to
58 TATA-less promoters and this led to the idea that TAFs could provide TFIID with additional
59 functional features(2, 3). Indeed, nine out of thirteen TAFs contain a histone fold domain
60 (HFD)(4) favoring the formation of TAF heterodimers. For instance, the TAF6-9 heterodimer
61 has been found to bind promoter elements downstream of the TATA-box(5-7) and is a direct
62 target of transcriptional activators(8, 9). Moreover, it has been shown that TAF knockouts
63 (KO) and *in vitro* TAF knock-down experiments result in both down- and up-regulated gene
64 expression of subsets of genes(10, 11). All these results together suggest that TFIID is a
65 highly flexible regulator of transcription, functioning both in gene activation and in
66 repression.

67 Additionally, co-activator complexes with histone acetyltransferase (HAT) activity
68 responsible for gene activation-associated interactions, including the ATAC (Ada-Two-A-
69 Containing) and SAGA (Spt-Ada-Gcn5-acetyltransferase) complexes, appear to have

70 distinct functional roles by targeting either promoters or enhancers or both (12) (and refs
71 therein).

72 TAF10 is a subunit of both the TFIID and the SAGA co-activator HAT complexes(13).
73 The role of TAF10 is indispensable for early embryonic transcription and mouse
74 development as knockout (KO) embryos die early in gestation between E3.5 and E5.5,
75 around the stage when the supply of maternal protein becomes insufficient(14). However,
76 when analyzing TFIID stability and transcription it was noted that not all cells and tissues
77 were equally affected by the loss of TAF10. For example, ablation of TAF10 in keratinocytes
78 impaired skin barrier formation and deregulated a subset of related genes when inactivated
79 during the fetal stage, but resulted in no detectable effect in adult keratinocytes(15).
80 Moreover, studies in which TAF10 was conditionally ablated in fetal or adult liver
81 demonstrated the essential role of TAF10 in liver development revealing the necessity of
82 TAF10 for TFIID stability to repress specific genes in the liver in postnatal life(10). These
83 findings together confirm that TAF10, probably as a subunit of TFIID and/or SAGA, is
84 essential during mouse development and suggest that TAF10 plays an important role during
85 embryonic development and homeostasis in a tissue-dependent manner. Understanding the
86 interplay of TAF10-containing TFIID and SAGA complexes with developmentally important
87 and tissue-specific transcription factors is crucial to obtain a more comprehensive view of
88 cell differentiation throughout development.

89 Erythropoiesis is the process by which red cells are formed(16). There are two waves of
90 erythropoiesis in mammals, primitive and definitive. Definitive erythropoiesis starts in the
91 fetal liver, and moves later during gestation to the spleen and bone marrow, which in mice
92 remain the sites of erythropoiesis during adulthood. The fetal and adult stages of definitive
93 erythropoiesis differ at the transcriptional level, exemplified in humans by the type of beta-
94 hemoglobin chain expressed. Many tissue-specific transcription factors have been studied
95 in order to provide mechanistic clues to this process of developmental-stage specific

96 hemoglobin expression(17). GATA1 is one of them, it is expressed in lineage-committed
97 cells (erythroid, megakaryocytic, eosinophilic, mast and dendritic cells) and plays an
98 important role in the regulation of differentiation and survival of these lineages(18, 19).
99 Embryos lacking *Gata1* die at approximately embryonic day 11.5 due to the maturation
100 arrest of primitive erythroid cells(20), while conditional knockout of *Gata1* in adults leads to
101 red cell aplasia and severe thrombocytopenia(21). However, the composition of general
102 transcription complexes, such as TFIID and SAGA, and the role of TAFs during
103 developmental erythropoiesis have not been investigated yet.

104 Alternative TFIID and other GTF complexes have been implicated in providing
105 alternative pathways leading to gene regulation during differentiation(22, 23). To gain
106 insight into the role of GTF in mouse erythropoiesis we have carried out specific inactivation
107 of TAF10, a cornerstone subunit of the TFIID and SAGA complexes(10), in the erythroid
108 compartment by crossing *TAF10lox*(14) with *EpoR-Cre* mice(24). We found that TAF10
109 ablation results in a block of erythropoiesis leading to severe anemia, which is lethal at
110 E13.5. Several GATA1 target genes, including *Gata1* itself, were deregulated when TAF10
111 was ablated. We have also analyzed the composition and stoichiometry of the TAF10-
112 containing transcription complexes, TFIID and SAGA, by mass spectrometry in proliferating
113 erythroid precursors (proerythroblasts) and synchronously differentiated erythroid cells of
114 mouse and human origin. Interestingly, we found that TAF10 interacts physically with the
115 master regulator of erythroid differentiation, the GATA1 transcription factor, and we
116 observed enrichment of TAF10 binding to the *GATA1* locus in human erythroid cells.
117 Collectively, these data suggest that the interaction of TAF10 with GATA1 is important to
118 facilitate the recruitment of TFIID and/or SAGA to GATA1-responsive promoters and that
119 the autologous control of GATA1 expression(25) requires the presence of TAF10 in these
120 complexes.

121

122 **Materials and Methods**

123 **Mice**

124 The *TAF10lox/KO*(14) mice and *EpoR-Cre*(24) mice have been described previously.
125 *TAF10lox/KO:EpoR-Cre^{+/-}* (TAF10KO^{cEry}) and single genetically modified mice were
126 maintained in a C57BL/6 background. All experiments described in this article have been
127 approved and conducted according to the animal welfare committee guidelines of Erasmus
128 MC Rotterdam.

129 **Human material**

130 Samples of fetal liver and buffy coats from peripheral blood were provided by the clinic and
131 the Sanquin Blood bank in The Netherlands, in compliance with the Erasmus MC Ethical
132 Guidelines Committee.

133 **Flow cytometry**

134 Fetal livers were dissected from embryos at E11.5, E12.5 and E13.5, and resuspended in
135 phosphate buffer saline (PBS) supplemented with 1% bovine serum albumin (BSA) to single
136 cell suspensions. Cells were stained on ice for 20 min and washed twice with PBS/1%BSA
137 before acquisition on a FACSARIAII instrument (Becton Dickinson, BD). Antibodies used for
138 staining include, TER119-PerCP-Cy5.5 (BD), KIT (CD117)-PECy7 (BD), CD71-PE (BD).
139 Since the *EpoR-Cre* allele includes a GFP reporter(24), EpoR-driven Cre expression was
140 followed by GFP in the FITC channel. Dead cells were excluded by Hoechst staining
141 (Invitrogen) and analysis was performed with the FlowJo software (Tree Star, Inc).

142 **Extract preparation and Immunoprecipitation (IP) Assays**

143 Nuclear extracts were prepared as described(10, 26). TAF10 immunoprecipitations (IPs)
144 were performed as described for mouse(10) and human cells(27). Mouse monoclonal
145 antibodies, 23TA 1H8(28) and 6TA 2B11(14), were used for human(29) and mouse TAF10
146 IPs, respectively, and a mix of 6TA 2B11 and 6TA 4G2 (27) (1/1000) against TAF10 protein

147 for assessment of IP efficiency by Western blotting. Mock IP was performed using a GST
148 antibody (Santa Cruz, sc-80004) according to the manufacturer's recommendations.

149 Mass spectrometry was performed as described before(30) on a LTQ-Orbitrap mass
150 spectrometer (Thermo).

151 **Purification of proteins**

152 GST-GATA1 and GST proteins (pGEX expression vectors) were expressed in BL21 *E. coli*
153 upon IPTG (0.4 mM) induction for 3 h at 30 °C. Bacteria were lysed (50 mM Tris-HCl pH 8.0,
154 400 mM NaCl, 5% Glycerol, 1mM Glutathione, 2,5 mM PMSF, 50 µg/ml DNase and 1 mM
155 MgCl₂, complete protease inhibitor cocktail (Roche)) and passed through the pressure
156 plunge three to four times. After centrifugation at 20.000 rpm for 20 min at 4 °C the extract
157 was incubated with pre-equilibrated (wash buffer without glutathione) glutathione beads
158 (Glutathione Sepharose 4B, GE Healthcare) for 1 h at room temperature (RT). After three
159 washes (50 mM Tris-HCl pH 8.0, 1 M NaCl, 5% Glycerol, 1 mM Glutathione, complete
160 protease inhibitor cocktail) the proteins were eluted (50 mM Glutathione, 50 mM Tris-HCl
161 pH 8.0, 150 mM NaCl, complete protease inhibitor cocktail).

162 **Chromatin immunoprecipitation (ChIP)**

163 Chromatin preparation from human erythroid progenitor cultures (HEPs) was previously
164 described(10). Fetal liver and adult HEPs were cultured(31) and used for ChIP reactions
165 that were performed as described(32) with the 23TA 1H8 antibody clone against the human
166 TAF10 protein, the GATA1 antibody (ab11852) and a CD71 antibody (347510, BD
167 Biosciences) as a negative control. qPCR was performed on the input and
168 immunoprecipitated samples using primers for the HS2 (palindromic GATA1 binding site) or
169 a more proximal GATA1 binding site at the GATA1 promoter. The relative fold-enrichment
170 was calculated using the delta delta Ct method(33) , setting the relative fold-enrichment of
171 CD71 background binding to 1. Primers used are Hs GATA1 palindromic binding site Fw 5'-
172 AGACTTATCTGCTGCCCCAG-3', Hs GATA1 palindromic binding site Rev 5'-

173 CCAGGCTAAGCCTGCAGGC-3' or Rev 5'-TAGAGCCTGTGGGATACCTTG-3'; Hs GATA1
174 binding site at -3kb Fw 5'- GGGATGAGGGAATAGTGGTG-3', Hs GATA1 binding site at -
175 3kb Rev 5'- GCTCTTTGTCTCTGTGTCTCTGTC-3'.

176 **Gene expression (RNA-seq and qRT-PCR)**

177 The RNA-seq library was generated according to the Illumina protocol using the TruSeq
178 RNA Sample Prep Kit v2 kit. 500ng of total RNA was initially extracted with Trizol Reagent
179 (Invitrogen) from mouse fetal livers of TAF10KO and WT embryos at E12.5. Quality of RNA
180 was checked with a Nanodrop analyzer and on an Agilent Technologies Bioanalyzer 2100.
181 Sequencing was performed on an Illumina HiSeq 2000 instrument. The reads were aligned
182 with Tophat version 2.0.8 [<http://genomebiology.com/2013/14/4/R36/abstract>] on the UCSC
183 mm10 reference genome using the Ensembl version 75 gene models(34).

184 **qRT-PCR**

185 cDNA synthesis was performed from 1µg of RNA with the DyNamo cDNA synthesis kit (F-
186 470, Finnzymes) and diluted to 10ng/µl concentration from which 10ng was used per
187 reaction at 20µl total volume. Conditions of the qRT-PCR and primer sequences are already
188 described(10) and reactions were performed in Applied Biosystems Thermal Real Time
189 PCR instruments (ABI 7900).

190 **RNA-Seq analysis**

191 Raw counts were measured with htseq-count version 0.6.0. using -m union -s no -a 20 as
192 settings(35). The counted data were normalized by the size factor of the libraries and
193 subsequently the Fragments Per Kilobase of exon per Million fragments mapped (FPKM)
194 were calculated. The differentially expressed genes were called using a generalized linear
195 negative binomial model that controlled for the effect of the RNA sample preparation date.
196 The calculations were performed by the DESeq2 R package(36). The False Discovery Rate
197 (FDR) was calculated with Benjamini Hochberg method(37) and the threshold value was set
198 to 0.01. Gene Ontology (GO) gene-enrichment analyses were carried out with the GO-stat

199 package(38) using a conditional hypergeometrical test for over-represented Ensembl Gene
200 IDs using a threshold p -value of 1×10^{-6} . The Principal Component Analysis (PCA) was
201 carried out using the Pearson's correlation matrix after blind variance stabilizing
202 transformation of the normalized counts(36).The RNA-seq data was joined with GATA1
203 ChIP-seq data(39) and plotted in a Venn diagram. The statistical package R was used for
204 calculations and plotting of the data (R Core Team (2014). R: A Language and Environment
205 for Statistical Computing. *Vienna, Austria: R Foundation for statistical computing*;
206 <http://www.r-project.org>.)

207 **Culture of erythroid cells**

208 Erythroid cell culture conditions have been described for mouse(40) and human erythroid
209 progenitors(31). Cells were kept under proliferation or differentiation conditions, and they
210 were followed by cell density and size monitoring with a CASY instrument (Innovatis, Roche
211 Diagnostics GmbH).

212

213 Results

214

215 Erythroid-specific knockout of TAF10 shows its requirement for erythropoiesis

216 To better understand the role of TFIID and SAGA in erythroid differentiation we generated
217 mice in which *TAF10* was specifically ablated in erythroid cells. *TAF10*^{+/-} mice are
218 normal(14), therefore we generated mice bearing a *TAF10* knockout allele and a *TAF10*
219 LoxP-flanked allele in order to reduce the recombination requirements to one allele when
220 generating conditional knockout mice. In order to study TAF10 loss-of-function specifically
221 in erythroid cells we generated *TAF10KO/Lox* animals bearing the erythroid-specific *EpoR*-
222 *Cre* allele(24), and we refer to them as *TAF10KO*^{cEry}. The expression of EpoR starts at E8.0
223 in yolk sac erythroid progenitors (41), increasing during definitive erythropoiesis in BFUE
224 and reaching maximal levels in CFUE progenitors.

225 Definitive erythropoiesis starts at E10.5 in the fetal liver but definitive erythroid cells
226 are detected in the circulation after E11.5, and only at E13.5 reach an approximate 1:1 ratio
227 with still circulating primitive erythroid cells derived from the yolk sac (42, 43). In order to
228 analyze this developmental transition period, we performed analysis of *TAF10KO*^{cEry} and
229 control embryos at E11.5, E12.5 and E13.5. From E12.5 onwards, *TAF10KO*^{cEry} embryos
230 were paler than control or heterozygous littermates and all *TAF10KO*^{cEry} embryos were
231 dead by E13.5. A representative picture of E12.5 embryos is shown in Figure 1A. Gross
232 morphological analysis revealed that the fetal liver size was considerably reduced at E12.5
233 in *TAF10KO*^{cEry} embryos when compared to control littermates (Figure 1A). The fetal liver
234 size and total blood cell counts were significantly reduced at E13.5 (Figure 1B). Flow
235 cytometry analysis of fetal liver cells showed a decrease in live cells at E13.5 (Figure 1C
236 and Table 1) in concordance with the apoptotic phenotype that has been shown previously
237 in other cell types lacking TAF10(10, 14). This decrease started to be noticeable at E12.5,
238 accompanied by reduced differentiation as measured by flow cytometry (see below). In

239 summary, erythroid-specific loss of TAF10 dramatically affected the erythroid compartment
240 between E12.5 and E13.5.

241 We next aimed to determine the differentiation stage at which TAF10 is essential
242 during the fetal erythroid differentiation process. Thus, we analyzed E11.5, E12.5 and E13.5
243 fetal livers by flow cytometry. Despite the fact that gross morphological analysis of E11.5
244 embryos revealed no significant differences, the distribution of the early erythroid markers
245 KIT and CD71 was altered in *TAF10KO^{cEry}* fetal livers when compared to control littermates,
246 and expression of Ter119 was significantly lower (Table 1). At this stage, the frequency of
247 KIT+ early progenitors was higher and the frequency of KIT+ CD71+ committed erythroid
248 progenitors as well as the more mature CD71+ cell population was reduced (Figure 2A), but
249 not as significant as observed at E12.5 (Table 1). By E12.5, both KIT+ early and
250 KIT+CD71+ committed erythroid progenitors had accumulated at the detriment of the more
251 mature KIT-CD71+ cells. By E13.5 there was an almost complete loss of KIT+CD71+ cells.
252 These data demonstrate a differentiation block of the erythroid progenitors in the fetal liver
253 throughout development. In addition, the KIT MFI (Mean Fluorescence Intensity) was higher
254 in *TAF10KO^{cEry}* fetal livers by E12.5, although not statistically significant, when compared to
255 control (see Figure 2C and Table 1). The CD71 MFI was reduced at E11.5, and was
256 significantly lower at E12.5 and E13.5 further supporting the notion of a differentiation
257 defect. The maturation delay and the reduction of mature cells (%KIT+, %CD71+,
258 %Ter119+cells, see Table 1) by E12.5 coincided with maximum expression of EpoR-Cre, as
259 measured by the expression of the GFP reporter of EpoR-Cre mice by flow cytometry
260 (Figure 3 and(24)). Furthermore, analysis of CD71 and Ter119 expression, as maturation
261 markers in erythroid cells, revealed a significant reduction in the mature CD71+Ter119+
262 fraction by E12.5 and a dramatic decrease by E13.5 (Figure 2B). The MFI of Ter119 was
263 reduced throughout development as measured from E11.5 to E13.5 (Figure 2C and Table
264 1). These data strongly suggest that erythroid development requires TAF10, and that

erythroid cells are blocked in differentiation upon TAF10 ablation. Since by E13.5 >80% of the fetal liver cells are mature erythroid cells (CD71⁺ Ter119⁺) in control embryos (Table 1), it is not surprising that *TAF10KO^{cEry}* embryos do not survive beyond this stage.

RNA-seq analysis of E12.5 *TAF10KO^{cEry}* fetal liver cells shows deregulation of several GATA1 target genes, including *Gata1* itself

To better characterize the TAF10-regulated genes in erythroid cells, we analyzed global gene expression levels by mRNA sequencing on E12.5 fetal liver cells from two homozygous *TAF10KO^{cEry}*, two heterozygous *TAF10KO^{cEry}* and three WT embryos. By using a principal component analysis (PCA) we observed a separate clustering of the homozygous *TAF10KO^{cEry}* fetal liver samples from the heterozygous *TAF10KO^{cEry}* and WT controls at E12.5 (Figure 4A). At this stage, when live erythroid cells are still present in the fetal liver, the gene expression analysis revealed around 300 deregulated genes with a minimum of 1.5 fold-change including the *Taf10* gene itself (Figure 4B & 4D). TAF10 levels, as expected, were reduced by more than 50% in *TAF10KO^{cEry}* fetal livers as compared to controls, which corresponds approximately to the percentage of erythroid cells (approx. 50%) beyond the KIT⁺ CD71⁺ committed erythroid progenitor stage in the KO fetal livers (Figure 2A and Table 1), when EpoR expression (and therefore Cre) reaches its maximum levels (as shown above in Figure 3). Gene Ontology analysis (GO) revealed that major 'metabolic pathways', 'cellular response to stress', 'cell type specific apoptosis' and 'cell death' related processes were among the most affected ones (Figure 4C). Expression levels of TFIID subunits were not significantly changed, consistent with previous analysis of TAF10 KO trophoblast and mouse fetal liver(10, 14), suggesting that the composition of the TFIID core complex containing five TAFs (TAF4, 5, 6, 9, 12)(44) does not change upon TAF10 loss. Similarly, the expression of the majority of the SAGA subunits was not affected with the exception of the *Trrap* and *Atxn7l1* genes which showed modest upregulation.

Initially, expression levels of the *Gata1*, *Gata2*, *Myb*, *Klf1*, and *Spi1* genes were measured by qRT-PCR (Figure 4D) and only *Gata1* and *Klf1* displayed a significant change in their expression levels. Subsequently, in the RNA-seq analysis we found that many of the differentially expressed genes are transcription factors and other erythroid-specific genes which have been recently identified as direct GATA1 targets by chromatin immunoprecipitation followed by sequencing (ChIP-seq) using E12.5 mouse fetal liver cells(39). We observed downregulation of genes encoding relevant transcription factors during erythropoiesis, such as *Gata1*, *Klf1*, *Nfe2*, *Zptba7*, *Bcl2l1* and other metabolically crucial erythroid genes including *Slc4a1*, *Gypa*, *Alas2*, *Car2* (Figure 5A, C). The genes encoding the TFDP22 coregulator, recently reported as an essential factor during terminal erythropoiesis, and the E2F2 transcription factor were significantly downregulated in *TAF10KO^{cEny}* together with two E2F2 target genes (*Dhfr*, *Ccna2*). We also found a subset of upregulated genes (*Spi1*, *Gata2*, *Runx1*, *Cux1*, *Car1*, *Rb1*, *Cbp/p300*, *Myc*), most of which are erythroid-related genes (Figure 5B&C). Of note, *Ddit3* and *Trib3*, which were recently reported to be co-induced during erythroid differentiation(45) and the *Ern1* gene, which has been linked to ER stress and induced apoptosis, were found significantly upregulated in the *TAF10* KO embryos (46-48). Important genes for erythroid differentiation, such as *Myb*, *Tal1*, *Cdk6* and the recently described *Exosc2* gene, part of the exosome complex (49), did not show any change in their expression levels (q-value >0.4). Most of the aforementioned genes were found to be bound by GATA1 in their regulatory sequences, but in many cases at different developmental stages (39, 45, 49, 50). Specifically for *Myb*, *Cdk6*, and *Exosc2* the GATA1 peaks were found below the cutoff value in E12.5 fetal liver (33).

The expression of globin genes (*Hbb-bh1*, *Hbb-y*, *Hbb-bt*, *Hbb-bs*, *Hba-a2*, *Hba-x*) was also lower in the *TAF10KO^{cEny}* fetal liver cells, and especially the *Hbb-y*, *Hba-a2* and *Hba-x* genes were found downregulated with high statistical power (Figure 5A & C). The *Hbb-bh1*

316 gene was the only one with no peaks for GATA1 binding at E12.5 among the affected globin
317 genes.

318 Interestingly, nine genes coding for the DNA-binding proteins (KRAB-ZFPs) shown
319 earlier (51) to be expressed in CD71+TER119+ and/or TER119+ erythroid cells (*Zfp689*,
320 *Zfp13*, *Zfp661*, *Zfp92*, *Zfp641*, *Zfp551*, *Zfp583*, *Zfp872*) appeared to be unaffected (q-val
321 >0.55) with the exception of *Zfp667* (q-val 0.02) expressed only in TER119+ cells and with
322 no identified GATA1 peak at E12.5, which was downregulated (Figure 5A). In addition,
323 TRIM28 that was recently reported to lead to a block in erythroid differentiation(51) when
324 deleted, did not change in expression, suggesting it is not implicated in the phenotype of the
325 embryos. Most of these genes had no or exceptionally one peak (i.e. *Zfp689*) for GATA1
326 binding, in their regulatory sequences (± 10 kb range around the TSS) at E12.5.

327 These results indicate that TAF10 ablation does not affect global expression as
328 observed before in hepatocyte-specific TAF10 KO cells(10). In addition, about half of the
329 deregulated genes in the *TAF10KO^{cEry}* are potential GATA1 target genes, with many of
330 them known to play a role during erythropoiesis (Figure 5D). In contrast, the expression of
331 genes that have a role in erythroid differentiation, but not bound by GATA1 at this
332 developmental stage (*Zfp689*, *Zfp13*, *Myb*, *Exosc8*), is not affected. Thus, GATA1 targets
333 are among the primary affected genes due to the loss of TAF10 in the *TAF10KO^{cEry}*
334 embryos *in vivo* suggesting an important requirement for a crosstalk or interaction between
335 GATA1 and TAF10.

336

337 **The composition of TAF10-containing complexes during erythroid differentiation and** 338 **development**

339 As several recent studies suggested that the composition of general transcription factor or
340 co-activator complexes may change during differentiation and development(22, 23) we
341 sought to analyze the composition of the TAF10-containing TFIID and SAGA complexes

342 during erythroid differentiation. To this end, protein extracts were prepared from mouse fetal
343 liver cell lines (m^{FLcl}) at the proerythroblast stage (immature), which are able to differentiate
344 to mature erythroblasts in a synchronous manner upon increasing the dose of
345 erythropoietin. TAF10-containing complexes were isolated by anti-TAF10
346 immunoprecipitations (IPs) from immature and differentiating (mature), but still nucleated,
347 erythroid cells and analyzed by mass spectrometry (MS). The relative abundance (emPAI:
348 exponentially modified Protein Abundance Index) of the different subunits in the isolated
349 complexes was first normalized by comparing all abundance values of the subunits of TFIID
350 to TAF1, or all the emPAI values of the subunits of SAGA to TRRAP, the largest subunits in
351 each respective complex (Figure 6A&B). Interestingly, when comparing the composition of
352 the TFIID complexes between proerythroblasts and mature erythroblasts, we noticed that
353 TAF4b completely disappeared from the TFIID complex of mature cells and also less TAF4
354 was associated with the TFIID complex in mature erythroid cells. In agreement with the
355 observation that TAF12 is the histone-fold partner of TAF4(52, 53), the TAF4/TAF4b
356 decrease in mature erythroid TFIID was accompanied by a reduction of TAF12. Note that
357 TAF9, but not TAF9b, was also significantly decreased in TAF10 IPs from mature erythroid
358 cell extracts. When comparing the composition of the SAGA complex at these two
359 differentiation stages after normalizing to TRRAP, we observed a slight reduction in several
360 subunits of SAGA complex in TAF10 IPs from mature erythroid cell extracts (Figure 6B).
361 Out of the two homologous SAGA HATs (GCN5 and PCAF), which have been reported to
362 be mutually exclusive in the corresponding SAGA complexes(54), the abundance of GCN5
363 is reduced about three times, while that of PCAF is not reduced, in mature erythroid cells.
364 Moreover, in the deubiquitination (DUB) module of SAGA, ATXN7 and its orthologue,
365 ATXN7L2 appear to be replaced by the orthologous ATXN7L1 at the mature stage. We note
366 that the absence of TAF13 from TFIID and of ENY2 from SAGA in these analyses may be
367 due to the very small size of these proteins.

368 Next, we sought to analyze the composition of human TAF10-containing complexes
369 during development (i.e. fetal and adult stages). Although the erythroid cells are at the
370 proerythroblast stage at both developmentally different niches (fetal and adult) and should
371 not be directly compared to the mouse situation we have made similar observations
372 regarding the slight stoichiometric changes that occur in the corresponding subunits of
373 TFIID and SAGA. Our analyses demonstrate that all of the subunits of the two complexes
374 are present in the corresponding complexes at these two developmental stages (Figure 6C,
375 D).

376 Importantly, these results together indicate that the canonical composition of the two
377 analyzed TAF10-containing complexes, TFIID and SAGA, does not change dramatically
378 during mouse and human erythroid differentiation and development. However, especially in
379 mouse complexes we observed often significant stoichiometric changes of those specific
380 subunits that have orthologues (TAF4/TAF4b, GCN5/PCAF, TAF9/TAF9b,
381 ATXN7/ATXN7L1/ATXNL2), which may slightly affect the function of these transcription
382 complexes.

383

384 **TAF10 and GATA1 interact in mouse and human fetal liver cells**

385 As our TAF10 KO experiments suggested a functional crosstalk between GATA1 and
386 TAF10, we next analyzed whether specific erythroid transcription factors, such as GATA1,
387 would co-immunoprecipitate with TAF10 from human fetal liver or human peripheral blood
388 erythroid progenitor cultures and mouse fetal liver cell lines. Importantly, GATA1, was
389 identified by mass spectrometry (MS) as a TAF10 interactor in h^{FL} cells together with other
390 previously reported activators and cofactors (Table 2), such as LDB1 and TAL1, which are
391 components of the so-called pentameric complex(55).

392 We also analyzed GATA1 interactors by carrying out an anti-GATA1 IP and
393 subsequent MS in MEL cells. Endogenous TAF10 together with other TAFs and SAGA

subunits were identified in the MS analysis (Table 3). Consequently, immunoprecipitation of GATA1 from MEL cells revealed that endogenous TAF10 co-immunoprecipitated with GATA1 and the Friend of GATA1 cofactor (FOG1) (Figure 7A). In addition, the interaction of endogenous TAF10 and GATA1 was verified by immunoprecipitating TAF10 from nuclear extracts prepared from MEL cells and the co-immunoprecipitated GATA1 was analyzed by Western blotting (Figure 7B). Similar IP assays were performed with E12.5 fetal liver cells or MEL cells that express biotinylated GATA1 (bio-GATA1) (Figure 8). These experiments further confirmed the interaction between TAF10-containing complexes and GATA1 previously identified in the MS data.

We further investigated whether the GATA1-TAF10 interaction is direct by *in vitro* protein-protein interaction experiments. First either TAF10 alone, or TAF8-TAF10 heterodimer was immune-purified using an anti-TAF10 antibody from SF9 extracts, in which the corresponding proteins were overexpressed using the baculovirus system. Next, purified GST-GATA1 protein or GST alone, were added to TAF10 or TAF10-TAF8 bound beads (Figure 7C). After several washing steps with high salt buffer, bead-bound proteins were denatured, resolved on a SDS-PAGE and analyzed by Western blotting using an anti-GST antibody. Our *in vitro* results indicate that GST-GATA1 bound to both TAF10- and TAF8-TAF10-containing beads, but GST alone did not (Figure 7D). These results together support a direct interaction between the key erythroid transcription factor GATA1 and TAF10.

TAF10 is bound to GATA1 sites in the GATA1 locus

In light of the downregulation of GATA1 mRNA levels we wished to determine whether TAF10 would be present, and thus possibly regulate the expression of the *GATA1* gene. We looked specifically at a palindromic GATA1 binding site known to be required for normal *GATA1* transcription, and an additional GATA1 binding site, which locates next to a TATA-

420 box at -3kb relative to the TSS(56, 57) (Figure 9A). We performed chromatin
421 immunoprecipitation (ChIP) of TAF10 and GATA1 in h^{FL} and h^{BL} cells representing two
422 distinct developmental stages as defined by the expression of fetal and adult hemoglobin
423 respectively. We found that TAF10 and GATA1 binding was more enriched at both GATA1
424 binding sites at the human GATA1 locus in the fetal liver as compared to adult blood
425 proerythroblasts (Figure 9B-C). However, while GATA1 binds at both binding sites
426 examined at both developmental stages, TAF10 is clearly not bound at the palindromic
427 GATA1 binding site in the adult stage and is significantly less enriched than GATA1 at the -
428 3kb binding site in the fetal stage (Figure 9C).

429 GATA1 auto-regulates its expression by binding to its own promoter and enhancers.
430 We detected TAF10-GATA1 protein-protein interaction mainly in h^{FL} extracts and ChIP
431 results show the selective binding of TAF10 at the palindromic GATA1 site during fetal
432 stages. Collectively, these results support the notion that TAF10 has a role in the
433 developmental regulation of GATA1 expression.

434

435 **Discussion**

436 Erythropoiesis is a process that is controlled tightly by the regulated expression of erythroid
437 specific transcription factors and their interactions with cofactors. General transcription
438 factors also have an active role, i.e. they have a more cell-type specific function than it was
439 originally thought(58). Whether the TAF10 component of TFIID and SAGA exerts such a
440 role by shaping the interactions with activators in erythroid differentiation and development
441 was the topic of this study.

442 TAF10 was specifically ablated to disrupt the canonical TFIID and SAGA complexes in
443 erythroid cells from early stages of mouse development (E8.0) in mice by crossing
444 *Taf10Lox* with *EpoR-Cre* mice. This resulted in a block in erythropoiesis leading to
445 embryonic death at around E13.5. A progressive delay in the differentiation kinetics through
446 development, which starts already at E11.5, is more pronounced at E12.5 with an
447 accumulation of CD71+TER119+ cells at the expense of mature TER119+ erythroid cells.
448 Expression analysis by mRNA sequencing (RNA-seq) showed that erythroid transcription
449 factor genes *Gata1*, *Klf1*, *Nfe2*, *Zbtb7a*, and *Bcl2l1* were within the downregulated group of
450 genes and expression of *Gata2*, *Spi1* and *Myb* did not change significantly, while *Runx1*,
451 *Rb1*, *Myc* and *Cited2* were upregulated following the opposite gene expression pattern that
452 characterizes the transition from the CD71+TER119+ towards to TER119+ mature erythroid
453 cells (59). Along the same lines, the TFDP2 coregulator and E2F2 transcription factor were
454 also found downregulated, and both genes were under the regulatory control of GATA1.
455 Normally, these two genes are induced upon erythroid differentiation and it was shown that
456 downregulation of *Tfdp2* prevents proper erythroid differentiation(45). Although *E2f2* was
457 downregulated significantly, the expression level of several E2F2 target genes was reduced
458 (*Dhfr*, *Ccna2*) in contrast to what we would expect due to the repressive role(45) of E2F2 on
459 its targets. Globin genes were also downregulated as a clear sign of the differentiation block
460 during erythroid differentiation. In contrast, genes with less well defined roles in the

erythroid lineage and no peaks for GATA1 in the ChIP-seq analysis at this developmental stage (E12.5), i.e. KRAB-ZFP proteins, did not change their expression levels in the *TAF10KO^{cEry}* fetal livers.

Nine of these KRAB-ZFP proteins are known to be expressed in erythroid progenitors and two of them are required for proper erythroid differentiation (ZFP689, ZFP13)(51). These results suggest that TAF10 is required to stabilize the PIC complex at certain loci, explaining why the transcription of specific genes is affected upon TAF10 loss. This finding is in agreement with the notion that TAF10 loss does not affect general transcription as would be expected for a cornerstone TAF of the TFIID(44). The specific gene expression changes in TAF10 KO erythroid cells could explain their progressive block in differentiation and subsequent apoptosis as identified by our GO analysis in *TAF10KO^{cEry}* fetal livers, since GATA1 KO erythroid cells are unable to differentiate but arrest their cell cycle and undergo apoptosis. In addition, three genes linked to ER stress and induced apoptosis (*Ddit3*(46), *Trib3*(60) and *Ern1*(48)), were found significantly upregulated in the *TAF10KO^{cEry}* fetal livers supporting the notion that apoptosis is among the main causes of the observed phenotype around E13.5.

In parallel with the *in vivo* studies we defined the composition of TAF10-containing complexes in erythroid cells in order to investigate the dynamic changes that appear to be crucial in other cell types during differentiation(61). We performed MS analysis of human and mouse cultured erythroid progenitor cells at an immature stage (proerythroblasts) and upon differentiation, which revealed that most of the TFIID and SAGA subunits are present in these complexes at all stages analyzed. Our data exclude a total rearrangement of the TFIID or SAGA complexes in this differentiation system, in contrast to what was reported for TFIID during liver hepatocyte(62) or myoblast differentiation(63). Nevertheless, we observe a dynamic reorganization of some TFIID and SAGA subunits, usually affecting those that have paralogues, such as TAF4/TAF4b, TAF9/TAF9b, GCN5/PCAF and

487 ATXN7/ATXN7L1/ATXN7L2, during differentiation without affecting the core structure of
488 these complexes. Interestingly, Pijnappel et al(64) demonstrated that overexpression of
489 TAF4 with the pluripotency factors, and presumably the incorporation of TAF4 into pre-
490 existing TFIID complexes lacking TAF4, can efficiently reprogram differentiated cells into
491 induced pluripotent stem cells (iPSCs). The TFIID complexes we purified from mouse
492 erythroid differentiated cells also have reduced TAF4/TAF12 heterodimers and no TAF4b,
493 whereas TAF4/TAF12 heterodimers and TAF4b are present at the immature stages of
494 differentiation. This is in excellent agreement with the results of the Timmers lab (51) and
495 suggests that the low level of TAF4 and/or the lack of TAF4b is associated with a
496 differentiated state, whereas immature stage cells contain a TFIID complex with
497 stoichiometric amounts of TAF4/4b.

498 The idea that developmental gene regulation is dependent on protein interactions
499 between TFIID, activators and co-activators is also supported by our results. GATA1 and its
500 well known partners LDB1 and TAL1 were found to interact with endogenous TAF10 in the
501 fetal liver cells of both mouse and human origin. This interaction was verified by reciprocal
502 immunoprecipitation (anti-TAF10 and anti-GATA1 IPs) in MEL cells and *in vitro* by using
503 purified GST-GATA1 and TAF10 (or TAF10-TAF8 heterodimers) proteins. Similar
504 interactions have been reported for activation of the β -globin gene between KLF1 and
505 TAF9(65) as well as GATA1 and MED1(66, 67) in erythroid cells.

506 Other TFs and co-factors, including subunits of the CCR4-NOT complex (e.g CNOT3),
507 CBX3 (a paralogue of CBX1 (HP1 β)) and TRIM28 were also found to interact with TAF10
508 by mass spectrometry (Table 2). CNOT3, CBX1 and TRIM28 were previously reported to
509 form a unique module involved in developmental processes(68) and TRIM28 in particular
510 has an important role in erythropoiesis(51, 69). Of note, CNOT3 and TRIM28 do not
511 physically interact, while there have been reports of interactions of TFIID with the CCR4-
512 NOT complex(70). Therefore, TFIID might be acting as a scaffold protein for the assembly

513 of the module and might play an important role in the developmental processes controlled
514 by this module, including erythropoiesis, which would be interesting to investigate in the
515 future.

516 Interestingly, our observation that TAF10 binding was enriched at the promoter of the
517 human GATA1 locus in fetal erythroid cells as compared to adult erythroid cells together
518 with the observed TAF10-GATA1 interaction suggest that there is a role for TAF10 in the
519 regulation of GATA1 transcription, which contributes to the phenotype observed in
520 *TAF10KO^{cEry}* embryos. This interaction preferentially occurs during the fetal stages of
521 erythropoiesis, indicating that it is a developmental-specific event exerting its effect mainly,
522 but not exclusively, on GATA1 target genes as observed in the RNA-seq data of the mouse
523 fetal livers. We know that GATA1 expression levels do not change in human fetal and adult
524 erythroblasts(71). However, there are dynamic changes in the occupancy of transcription
525 factors and consequently in protein-protein interactions, involving master regulators, that
526 could potentially activate, repress(72) or stabilize gene expression levels. When such
527 interactions are disturbed, transcriptional deregulation is not global but it depends on the
528 transcriptional state of the gene at that developmental stage(10).

529 We propose that TFIID and SAGA contribute to this dynamic landscape of
530 developmental-specific protein interactions through TAF10 interaction with GATA1 thus
531 contributing to development and differentiation of the erythroid lineage.

532

533 **Acknowledgements**

534 The authors would like to thank the PRIDE team for their help and support regarding the
535 deposition of the mass spectrometry data. The mass spectrometry proteomics data have
536 been deposited to the
537 ProteomeXchange Consortium (<http://proteomecentral.proteomexchange.org>) via the
538 PRIDE partner repository [1] with the dataset identifier PXD000729 and DOI
539 10.6019/PXD000729. The GST and GST-GATA1 plasmids were a generous gift from K.
540 Freson at KU Leuven (Molecular and Vascular Biology). We are also grateful to the
541 members of T. Economou lab (Molecular Bacteriology) at KU Leuven and especially to N.
542 Famelis and K. Tsolis for helping with the purification of the GST fusion proteins and Petros
543 Kolovos from Erasmus MC for technical support.

544 This work has been supported partially by an EMBO short-term fellowship ASTF 15-2010
545 (P.P.), the Netherlands Organization for Scientific Research (NWO-VENI 863.09.012, L.G.),
546 the Netherlands Genomics Initiative (NGI Zenith 93511036), the Netherlands Proteomics
547 Center (NPC), the Netherlands Initiative of Regenerative Medicine (NIRM) and the EU
548 Integrated project EuTRACC to F.G. and L.T.; the Landsteiner Foundation for Blood
549 Transfusion Research (LSBR; 1040) to FG and SP; ZonMw (TOP 40-00812-98-12128 and
550 DN 82-301), EU FP7 Specific Cooperation Research Project "THALAMOSS" (306201) to
551 S.P. and ERC Advanced (Birtoaction, N° 340551) grant to L.T.

552 Contribution: P.P., F.G., and L.T. designed the study; P.P., L.G., J.D., D.N.P., E.K., R.vdL.,
553 F.P., E.S., performed the experiments; P.P., L.G., J.D., H.J.G.vdW., D.H.W.D., P.V., J.S.,
554 S.P., F.G., L.T. analyzed the data; P.P., L.G., S.P., F.G., L.T. wrote the paper.

555

556 **References**

- 557 1. **Muller F, Tora L.** 2013. Chromatin and DNA sequences in defining promoters for
558 transcription initiation. *Biochimica et biophysica acta* doi:10.1016/j.bbagr.2013.11.003.
- 559 2. **Gershenson NI, Ioshikhes IP.** 2005. Synergy of human Pol II core promoter elements
560 revealed by statistical sequence analysis. *Bioinformatics* **21**:1295-1300.
- 561 3. **Zhang MQ.** 1998. Identification of human gene core promoters in silico. *Genome research*
562 **8**:319-326.
- 563 4. **Gangloff YG, Romier C, Thuault S, Werten S, Davidson I.** 2001. The histone fold is a key
564 structural motif of transcription factor TFIID. *Trends in biochemical sciences* **26**:250-257.
- 565 5. **Kaufmann J, Smale ST.** 1994. Direct recognition of initiator elements by a component of
566 the transcription factor IID complex. *Genes Dev* **8**:821-829.
- 567 6. **Chalkley GE, Verrijzer CP.** 1999. DNA binding site selection by RNA polymerase II TAFs:
568 a TAF(II)250-TAF(II)150 complex recognizes the initiator. *EMBO J* **18**:4835-4845.
- 569 7. **Juven-Gershon T, Kadonaga JT.** 2010. Regulation of gene expression via the core
570 promoter and the basal transcriptional machinery. *Dev Biol* **339**:225-229.
- 571 8. **Vassallo MF, Tanese N.** 2002. Isoform-specific interaction of HP1 with human TAFII130.
572 *Proc Natl Acad Sci U S A* **99**:5919-5924.
- 573 9. **Liu WL, Coleman RA, Ma E, Grob P, Yang JL, Zhang Y, Dailey G, Nogales E, Tjian R.**
574 2009. Structures of three distinct activator-TFIID complexes. *Genes Dev* **23**:1510-1521.
- 575 10. **Tatarakis A, Margaritis T, Martinez-Jimenez CP, Kouskouti A, Mohan WS, 2nd,**
576 **Haroniti A, Kafetzopoulos D, Tora L, Talianidis I.** 2008. Dominant and redundant
577 functions of TFIID involved in the regulation of hepatic genes. *Mol Cell* **31**:531-543.
- 578 11. **Frontini M, Soutoglou E, Argentini M, Bole-Feysot C, Jost B, Scheer E, Tora L.** 2005.
579 TAF9b (formerly TAF9L) is a bona fide TAF that has unique and overlapping roles with
580 TAF9. *Mol Cell Biol* **25**:4638-4649.
- 581 12. **Spedale G, Timmers HT, Pijnappel WW.** 2012. ATAC-king the complexity of SAGA
582 during evolution. *Genes & development* **26**:527-541.
- 583 13. **Timmers HT, Tora L.** 2005. SAGA unveiled. *Trends Biochem Sci* **30**:7-10.
- 584 14. **Mohan WS, Jr., Scheer E, Wendling O, Metzger D, Tora L.** 2003. TAF10 (TAF(II)30) is
585 necessary for TFIID stability and early embryogenesis in mice. *Mol Cell Biol* **23**:4307-4318.
- 586 15. **Indra AK, Mohan WS, 2nd, Frontini M, Scheer E, Messaddeq N, Metzger D, Tora L.**
587 2005. TAF10 is required for the establishment of skin barrier function in foetal, but not in
588 adult mouse epidermis. *Dev Biol* **285**:28-37.
- 589 16. **Wong PM, Chung SW, Eaves CJ, Chui DH.** 1985. Ontogeny of the mouse hemopoietic
590 system. *Prog Clin Biol Res* **193**:17-28.
- 591 17. **Sankaran VG, Xu J, Orkin SH.** 2010. Advances in the understanding of haemoglobin
592 switching. *Br J Haematol* **149**:181-194.
- 593 18. **Ferreira R, Ohneda K, Yamamoto M, Philipsen S.** 2005. GATA1 function, a paradigm for
594 transcription factors in hematopoiesis. *Mol Cell Biol* **25**:1215-1227.
- 595 19. **Gutierrez L, Nikolic T, van Dijk TB, Hammad H, Vos N, Willart M, Grosveld F,**
596 **Philipsen S, Lambrecht BN.** 2007. Gata1 regulates dendritic-cell development and survival.
597 *Blood* **110**:1933-1941.
- 598 20. **Fujiwara Y, Browne CP, Cunniff K, Goff SC, Orkin SH.** 1996. Arrested development of
599 embryonic red cell precursors in mouse embryos lacking transcription factor GATA-1. *Proc*
600 *Natl Acad Sci U S A* **93**:12355-12358.
- 601 21. **Gutierrez L, Tsukamoto S, Suzuki M, Yamamoto-Mukai H, Yamamoto M, Philipsen S,**
602 **Ohneda K.** 2008. Ablation of Gata1 in adult mice results in aplastic crisis, revealing its
603 essential role in steady-state and stress erythropoiesis. *Blood* **111**:4375-4385.
- 604 22. **Muller F, Zaucker A, Tora L.** 2010. Developmental regulation of transcription initiation:
605 more than just changing the actors. *Curr Opin Genet Dev* **20**:533-540.

- 606 23. **Goodrich JA, Tjian R.** 2010. Unexpected roles for core promoter recognition factors in cell-
607 type-specific transcription and gene regulation. *Nat Rev Genet* **11**:549-558.
- 608 24. **Heinrich AC, Pelanda R, Klingmuller U.** 2004. A mouse model for visualization and
609 conditional mutations in the erythroid lineage. *Blood* **104**:659-666.
- 610 25. **Tsai SF, Strauss E, Orkin SH.** 1991. Functional analysis and in vivo footprinting implicate
611 the erythroid transcription factor GATA-1 as a positive regulator of its own promoter. *Genes*
612 *Dev* **5**:919-931.
- 613 26. **Demeny MA, Soutoglou E, Nagy Z, Scheer E, Janoshazi A, Richardot M, Argenti M,**
614 **Kessler P, Tora L.** 2007. Identification of a small TAF complex and its role in the assembly
615 of TAF-containing complexes. *PLoS One* **2**:e316.
- 616 27. **Jacq X, Brou C, Lutz Y, Davidson I, Chambon P, Tora L.** 1994. Human TAFII30 is
617 present in a distinct TFIID complex and is required for transcriptional activation by the
618 estrogen receptor. *Cell* **79**:107-117.
- 619 28. **Wieczorek E, Brand M, Jacq X, Tora L.** 1998. Function of TAF(II)-containing complex
620 without TBP in transcription by RNA polymerase II. *Nature* **393**:187-191.
- 621 29. **Soutoglou E, Demeny MA, Scheer E, Fienga G, Sassone-Corsi P, Tora L.** 2005. The
622 nuclear import of TAF10 is regulated by one of its three histone fold domain-containing
623 interaction partners. *Mol Cell Biol* **25**:4092-4104.
- 624 30. **van den Berg DL, Snoek T, Mullin NP, Yates A, Bezstarosti K, Demmers J, Chambers I,**
625 **Poot RA.** 2010. An Oct4-centered protein interaction network in embryonic stem cells. *Cell*
626 *stem cell* **6**:369-381.
- 627 31. **Leberbauer C, Boulme F, Unfried G, Huber J, Beug H, Mullner EW.** 2005. Different
628 steroids co-regulate long-term expansion versus terminal differentiation in primary human
629 erythroid progenitors. *Blood* **105**:85-94.
- 630 32. **Follows GA, Tagoh H, Lefevre P, Hodge D, Morgan GJ, Bonifer C.** 2003. Epigenetic
631 consequences of AML1-ETO action at the human c-FMS locus. *EMBO J* **22**:2798-2809.
- 632 33. **Schmittgen TD, Livak KJ.** 2008. Analyzing real-time PCR data by the comparative C(T)
633 method. *Nat Protoc* **3**:1101-1108.
- 634 34. **Flicek P, Amode MR, Barrell D, Beal K, Billis K, Brent S, Carvalho-Silva D, Clapham**
635 **P, Coates G, Fitzgerald S, Gil L, Giron CG, Gordon L, Hourlier T, Hunt S, Johnson N,**
636 **Juettemann T, Kahari AK, Keenan S, Kulesha E, Martin FJ, Maurel T, McLaren WM,**
637 **Murphy DN, Nag R, Overduin B, Pignatelli M, Pritchard B, Pritchard E, Riat HS,**
638 **Ruffier M, Sheppard D, Taylor K, Thormann A, Trevanion SJ, Vullo A, Wilder SP,**
639 **Wilson M, Zadissa A, Aken BL, Birney E, Cunningham F, Harrow J, Herrero J,**
640 **Hubbard TJ, Kinsella R, Muffato M, Parker A, Spudich G, Yates A, et al.** 2014. Ensembl
641 2014. *Nucleic acids research* **42**:D749-755.
- 642 35. **Anders S, Pyl PT, Huber W.** 2014. HTSeq - A Python framework to work with high-
643 throughput sequencing data. *Bioinformatics* doi:10.1093/bioinformatics/btu638.
- 644 36. **Anders S, Huber W.** 2010. Differential expression analysis for sequence count data. *Genome*
645 *Biol* **11**:R106.
- 646 37. **Hochberg Y, Benjamini Y.** 1990. More powerful procedures for multiple significance
647 testing. *Statistics in medicine* **9**:811-818.
- 648 38. **Falcon S, Gentleman R.** 2007. Using GOSTats to test gene lists for GO term association.
649 *Bioinformatics* **23**:257-258.
- 650 39. **Papadopoulos GL, Karkoulia E, Tsamardinos I, Porcher C, Ragoussis J, Bungert J,**
651 **Strouboulis J.** 2013. GATA-1 genome-wide occupancy associates with distinct epigenetic
652 profiles in mouse fetal liver erythropoiesis. *Nucleic acids research* **41**:4938-4948.
- 653 40. **von Lindern M, Deiner EM, Dolznig H, Parren-Van Amelsvoort M, Hayman MJ,**
654 **Mullner EW, Beug H.** 2001. Leukemic transformation of normal murine erythroid
655 progenitors: v- and c-ErbB act through signaling pathways activated by the EpoR and c-Kit in
656 stress erythropoiesis. *Oncogene* **20**:3651-3664.

- 657 41. **Lee R, Kertesz N, Joseph SB, Jegalian A, Wu H.** 2001. Erythropoietin (Epo) and EpoR
658 expression and 2 waves of erythropoiesis. *Blood* **98**:1408-1415.
- 659 42. **Isern J, Fraser ST, He Z, Baron MH.** 2010. Developmental niches for embryonic erythroid
660 cells. *Blood Cells Mol Dis* **44**:207-208.
- 661 43. **Palis J.** 2014. Primitive and definitive erythropoiesis in mammals. *Front Physiol* **5**:3.
- 662 44. **Bieniossek C, Papai G, Schaffitzel C, Garzoni F, Chaillet M, Scheer E, Papadopoulos P,**
663 **Tora L, Schultz P, Berger I.** 2013. The architecture of human general transcription factor
664 TFIID core complex. *Nature* **493**:699-702.
- 665 45. **Chen C, Lodish HF.** 2014. Global analysis of induced transcription factors and cofactors
666 identifies Tfdp2 as an essential coregulator during terminal erythropoiesis. *Exp Hematol*
667 **42**:464-476 e465.
- 668 46. **Lu M, Lawrence DA, Marsters S, Acosta-Alvear D, Kimmig P, Mendez AS, Paton AW,**
669 **Paton JC, Walter P, Ashkenazi A.** 2014. Cell death. Opposing unfolded-protein-response
670 signals converge on death receptor 5 to control apoptosis. *Science* **345**:98-101.
- 671 47. **Harding HP, Zhang Y, Ron D.** 1999. Protein translation and folding are coupled by an
672 endoplasmic-reticulum-resident kinase. *Nature* **397**:271-274.
- 673 48. **Brewer JW, Hendershot LM, Sherr CJ, Diehl JA.** 1999. Mammalian unfolded protein
674 response inhibits cyclin D1 translation and cell-cycle progression. *Proc Natl Acad Sci U S A*
675 **96**:8505-8510.
- 676 49. **McIver SC, Kang YA, DeVilbiss AW, O'Driscoll CA, Ouellette JN, Pope NJ,**
677 **Camprecios G, Chang CJ, Yang D, Bouhassira EE, Ghaffari S, Bresnick EH.** 2014. The
678 exosome complex establishes a barricade to erythroid maturation. *Blood* **124**:2285-2297.
- 679 50. **Yu M, Riva L, Xie H, Schindler Y, Moran TB, Cheng Y, Yu D, Hardison R, Weiss MJ,**
680 **Orkin SH, Bernstein BE, Fraenkel E, Cantor AB.** 2009. Insights into GATA-1-mediated
681 gene activation versus repression via genome-wide chromatin occupancy analysis. *Mol Cell*
682 **36**:682-695.
- 683 51. **Barde I, Rauwel B, Marin-Florez RM, Corsinotti A, Laurenti E, Verp S, Offner S,**
684 **Marquis J, Kapopoulou A, Vanicek J, Trono D.** 2013. A KRAB/KAP1-miRNA cascade
685 regulates erythropoiesis through stage-specific control of mitophagy. *Science* **340**:350-353.
- 686 52. **Gangloff YG, Werten S, Romier C, Carre L, Poch O, Moras D, Davidson I.** 2000. The
687 human TFIID components TAF(II)135 and TAF(II)20 and the yeast SAGA components
688 ADA1 and TAF(II)68 heterodimerize to form histone-like pairs. *Molecular and cellular*
689 *biology* **20**:340-351.
- 690 53. **Leurent C, Sanders S, Ruhlmann C, Mallouh V, Weil PA, Kirschner DB, Tora L,**
691 **Schultz P.** 2002. Mapping histone fold TAFs within yeast TFIID. *EMBO J* **21**:3424-3433.
- 692 54. **Nagy Z, Riss A, Fujiyama S, Krebs A, Orpinell M, Jansen P, Cohen A, Stunnenberg**
693 **HG, Kato S, Tora L.** 2010. The metazoan ATAC and SAGA coactivator HAT complexes
694 regulate different sets of inducible target genes. *Cellular and molecular life sciences : CMLS*
695 **67**:611-628.
- 696 55. **Soler E, Andrieu-Soler C, de Boer E, Bryne JC, Thongjuea S, Stadhouders R, Palstra**
697 **RJ, Stevens M, Kockx C, van Ijcken W, Hou J, Steinhoff C, Rijkers E, Lenhard B,**
698 **Grosveld F.** 2010. The genome-wide dynamics of the binding of Ldb1 complexes during
699 erythroid differentiation. *Genes Dev* **24**:277-289.
- 700 56. **Nicolis S, Bertini C, Ronchi A, Crotta S, Lanfranco L, Moroni E, Giglioni B, Ottolenghi**
701 **S.** 1991. An erythroid specific enhancer upstream to the gene encoding the cell-type specific
702 transcription factor GATA-1. *Nucleic Acids Res* **19**:5285-5291.
- 703 57. **Moriguchi T, Yu L, Takai J, Hayashi M, Satoh H, Suzuki M, Ohneda K, Yamamoto M.**
704 2015. The Human GATA1 Gene Retains a 5' Insulator that Maintains Chromosomal
705 Architecture and GATA1 Expression Levels in Splenic Erythroblasts. *Mol Cell Biol*
706 doi:10.1128/MCB.00011-15.
- 707 58. **Naar AM, Lemon BD, Tjian R.** 2001. Transcriptional coactivator complexes. *Annual*
708 *review of biochemistry* **70**:475-501.

- 709 59. **Wong P, Hattangadi SM, Cheng AW, Frampton GM, Young RA, Lodish HF.** 2011.
710 Gene induction and repression during terminal erythropoiesis are mediated by distinct
711 epigenetic changes. *Blood* **118**:e128-138.
- 712 60. **Ohoka N, Yoshii S, Hattori T, Onozaki K, Hayashi H.** 2005. TRB3, a novel ER stress-
713 inducible gene, is induced via ATF4-CHOP pathway and is involved in cell death. *EMBO J*
714 **24**:1243-1255.
- 715 61. **Liu Z, Scannell DR, Eisen MB, Tjian R.** 2011. Control of embryonic stem cell lineage
716 commitment by core promoter factor, TAF3. *Cell* **146**:720-731.
- 717 62. **D'Alessio JA, Ng R, Willenbring H, Tjian R.** 2011. Core promoter recognition complex
718 changes accompany liver development. *Proc Natl Acad Sci U S A* **108**:3906-3911.
- 719 63. **Deato MD, Tjian R.** 2007. Switching of the core transcription machinery during myogenesis.
720 *Genes & development* **21**:2137-2149.
- 721 64. **Pijnappel WW, Esch D, Baltissen MP, Wu G, Mischerikow N, Bergsma AJ, van der Wal
722 E, Han DW, Bruch H, Moritz S, Lijnzaad P, Altelaar AF, Sameith K, Zaehres H, Heck
723 AJ, Holstege FC, Scholer HR, Timmers HT.** 2013. A central role for TFIID in the
724 pluripotent transcription circuitry. *Nature* **495**:516-519.
- 725 65. **Sengupta T, Cohet N, Morle F, Bieker JJ.** 2009. Distinct modes of gene regulation by a
726 cell-specific transcriptional activator. *Proc Natl Acad Sci U S A* **106**:4213-4218.
- 727 66. **Stumpf M, Waskow C, Krotschel M, van Essen D, Rodriguez P, Zhang X, Guyot B,
728 Roeder RG, Borggreffe T.** 2006. The mediator complex functions as a coactivator for
729 GATA-1 in erythropoiesis via subunit Med1/TRAP220. *Proc Natl Acad Sci U S A*
730 **103**:18504-18509.
- 731 67. **Stumpf M, Yue X, Schmitz S, Luche H, Reddy JK, Borggreffe T.** 2010. Specific erythroid-
732 lineage defect in mice conditionally deficient for Mediator subunit Med1. *Proc Natl Acad Sci*
733 *U S A* **107**:21541-21546.
- 734 68. **Hu G, Kim J, Xu Q, Leng Y, Orkin SH, Elledge SJ.** 2009. A genome-wide RNAi screen
735 identifies a new transcriptional module required for self-renewal. *Genes Dev* **23**:837-848.
- 736 69. **Hosoya T, Clifford M, Losson R, Tanabe O, Engel JD.** 2013. TRIM28 is essential for
737 erythroblast differentiation in the mouse. *Blood* **122**:3798-3807.
- 738 70. **Collart MA, Timmers HT.** 2004. The eukaryotic Ccr4-not complex: a regulatory platform
739 integrating mRNA metabolism with cellular signaling pathways? *Prog Nucleic Acid Res Mol*
740 *Biol* **77**:289-322.
- 741 71. **Xu J, Shao Z, Glass K, Bauer DE, Pinello L, Van Handel B, Hou S, Stamatoyannopoulos
742 JA, Mikkola HK, Yuan GC, Orkin SH.** 2012. Combinatorial assembly of developmental
743 stage-specific enhancers controls gene expression programs during human erythropoiesis.
744 *Developmental cell* **23**:796-811.
- 745 72. **Pimkin M, Kossenkova AV, Mishra T, Morrissey CS, Wu W, Keller CA, Blobel GA, Lee
746 D, Beer MA, Hardison RC, Weiss MJ.** 2014. Divergent functions of hematopoietic
747 transcription factors in lineage priming and differentiation during erythro-megakaryopoiesis.
748 *Genome research* doi:10.1101/gr.164178.113.
- 749
- 750

751 **Figure legends**

752

753 **Figure 1. Developmental analysis of *TAF10KO^{cEry}***

754 **A.** Representative pictures of control and *TAF10KO^{cEry}* embryos at E12.5. *TAF10KO^{cEry}*
755 embryos are pale and the fetal liver is much smaller compared to those of the control
756 embryos.

757 **B.** Cell count numbers at E13.5 from fetal liver and embryonic blood of control and
758 *TAF10KO^{cEry}* embryos.

759 **C.** Flow cytometry analysis of fetal liver single cell suspensions of control and *TAF10KO^{cEry}*
760 embryos at different developmental stages (E11.5, E12.5 and E13.5). Numbers indicate the
761 percentages of live cells (Hoechst negative).

762

763 **Figure 2. Flow cytometry of *TAF10KO^{cEry}* fetal liver cells during gestation**

764 Representative flow cytometry analysis of fetal liver single cell suspension of control and
765 *TAF10KO^{cEry}* embryos at E11.5, E12.5 and E13.5 following the differentiation of erythroid
766 cells.

767 **A.** Staining with KIT and CD71 markers (numbers indicate percentages of gated live cells).

768 **B.** Staining with CD71 and Ter119 markers (numbers indicate percentages of gated live
769 cells).

770 **C.** MFI (Mean Fluorescence Intensity) graphs of KIT, CD71 and Ter119 populations as
771 expressed during development of erythroid cells of control and *TAF10KO^{cEry}* fetal liver cells.

772

773

774 **Figure 3. Analysis of *EpoR-Cre* transgenic expression**

775 Flow cytometry analysis of fetal livers cells following the expression of the GFP protein
776 expressed in frame with Cre recombinase in *EpoR-Cre* mice. Expression of GFP confined

777 to the erythroid compartment was detected initially in KIT+/CD71+ cells at E11.5 (green
778 population for controls and red population for *TAF10KO^{cEry}* erythroid cells). Erythroid cells
779 are affected in *TAF10KO^{cEry}* embryos and that is why the percentage (numbers shown in
780 the graphs) of CD71+/GFP+ cells is lower as compared to control cells at E12.5. By E13.5
781 most of the cells are dead.

782

783 **Figure 4. Gene Expression analysis of E12.5 *TAF10KO^{cEry}* fetal livers**

784 **A.** Principal Component analysis (PCA) plot of the first two components of the RNA-seq
785 fetal liver samples (*TAF10KO^{cEry}*, Heterozygous *TAF10KO*, WT). The variance explained by
786 each component is depicted between parenthesis on the axes.

787 **B.** MA-plot of the mean normalized gene count versus the log₂ fold changes of
788 *TAF10KO^{cEry}* over WT and Heterozygous *TAF10KO*. Genes are plotted as closed black
789 circles. Genes with an adjusted *p*-value (FDR) < 0.01 are colored red. Genes that fall out of
790 the window boundaries of -2 or 2 log₂ fold change are plotted as open triangles.

791 **C.** Gene ontology (GO) analysis of the upregulated genes in the *TAF10KO^{cEry}* fetal livers.
792 Metabolic pathways, apoptotic and cell death related processes and proliferation are among
793 the most affected.

794 **D.** qRT-PCR on total mRNA of fetal liver cells at E12.5. Expression levels of transcription
795 factors and globin genes are depicted. Bars represent standard error of the mean (SEM).

796

797 **Figure 5. Gene Expression analysis (Transcription factors, erythroid-related and**
798 **globin genes)**

799 **A.** RNA-seq gene expression levels (FPKM: Fragments Per Kilobase of exon per Million
800 fragments mapped) of upregulated erythroid-related genes with a *q*-value<0.05 and GATA1
801 binding peaks found within ±10Kb of their TSS ,

802 **B.** Downregulated genes with a *q*-value<0.05 with GATA1 binding peaks found,

803 **C.** Deregulated genes with a q-value>0.05 with GATA1 binding peaks found, and
804 **D.** Venn diagram of deregulated genes (upreg: upregulated in *TAF10KO^{cEry}* fetal liver cells-
805 green circle, downreg: downregulated genes in *TAF10KO^{cEry}* fetal liver cells-purple circle)
806 as identified by RNA-seq analysis (q-value <0.05) and GATA1 target genes described in
807 (39)(red circle). Half of the deregulated genes have at least one GATA1 binding peak at
808 ± 10 Kb of their TSS.

809

810 **Figure 6. Mass spectrometry of TFIID and SAGA complexes in mouse and human**
811 **erythroid cells**

812 **A and B.** TAF10-containing complexes, TFIID (in A) and SAGA (in B), were isolated by a
813 TAF10 immunoprecipitation from protein extracts prepared from immature and
814 differentiating (mature) mouse erythroid cells and analyzed by mass spectrometry. The
815 relative abundance (emPAI: exponentially modified Protein Abundance Index) values of the
816 different subunits in the isolated complexes were first normalized by comparing the
817 abundance values of all the subunits of TFIID to TAF1, or all the subunits of SAGA to
818 TRRAP, the largest subunits in each complex.

819 **C and D.** Similarly, TAF10-containing complexes, TFIID (in C) and SAGA (in D), were
820 isolated by a TAF10 immunoprecipitation from protein extracts prepared from human fetal
821 liver (hFL) and human peripheral blood erythroid progenitors (hBL) and analyzed by mass
822 spectrometry. The emPAI values presented were normalized as described for the mouse
823 samples.

824

825 **Figure 7. Immunoprecipitation of TAF10 and GATA1 in MEL cells**

826 **A.** GATA1 immunoprecipitation in MEL cells. Anti-GATA1 antibody (N6) was used for
827 Western blot analysis. TAF10 and FOG-1 are co-immunoprecipitated.

828 **B.** TAF10 immunoprecipitation in MEL nuclear extracts using the 6TA 2B11 antibody clone.
829 IgG antibody was used as a control. GATA1 is detected in the IP fraction, confirming the MS
830 results. Sup: supernatant.

831 **C.** TAF10 alone, or TAF8-TAF10 heterodimer was immune-purified using an anti-TAF10
832 antibody from SFf9 extracts and tested by Western blot using the indicated antibodies.
833 GST-GATA1 protein, or GST, were also purified and tested by coomassie blue (CBB)
834 staining.

835 **D.** The purified proteins were combined as indicated, incubated and after several washes
836 the beads-bound proteins were denatured, resolved on a SDS-PAGE and analyzed by
837 Western blot using an anti- GST antibody. Antibody heavy (AbHc) and light (AbLc) chains
838 are indicated.

839

840 **Figure 8. Immunoprecipitations of TAF10 and GATA1 in MEL cells and mouse fetal**
841 **liver E12.5**

842 **A.** MEL cells and mouse fetal liver nuclear cell extracts were used to immunoprecipitate
843 GATA1 endogenous protein or the bio-GATA1 over-expressed (O/E) in MEL cells. GATA1
844 (N6) IP or streptavidin pulldown co-immunoprecipitates GATA1/bio-GATA1 and TAF10
845 protein as detected by Western blot assays using M20 (GATA1) and 6TA 2B11 (TAF10)
846 antibodies. BirA MEL cells were used as controls.

847 **B.** TAF10 (6TA 2B11) IP in bio-GATA1 O/E MEL cells co-immunoprecipitates GATA1 in the
848 reverse IP.

849

850 **Figure 9. ChIP assays of TAF10 and GATA1 in the GATA1 locus in h^{FL} and h^{BL}**

851 A TAF10 antibody (23TA 1H8 mAb) and a GATA1 antibody were used to immunoprecipitate
852 the formaldehyde-crosslinked chromatin from h^{FL} and h^{PB} erythroid progenitor cells.

853 **A.** Primers for GATA1 binding sites of the human GATA1 locus, as indicated (palindromic
854 GATA1 binding site and GATA1 binding site at -3kb region relative to the TSS), were used
855 to estimate the relative fold enrichment (RFE) of TAF10 and GATA1 by qRT-PCR. A CD71
856 antibody (isotype control) was used for the mock IP and background enrichment was set to
857 value 1.

858 **B.** Enrichment for TAF10 and GATA1 at both binding sites of interest is shown in
859 independent experiments for fetal liver and adult blood.

860 Overview of all ChIP experiments. See panel A for positions of primers.

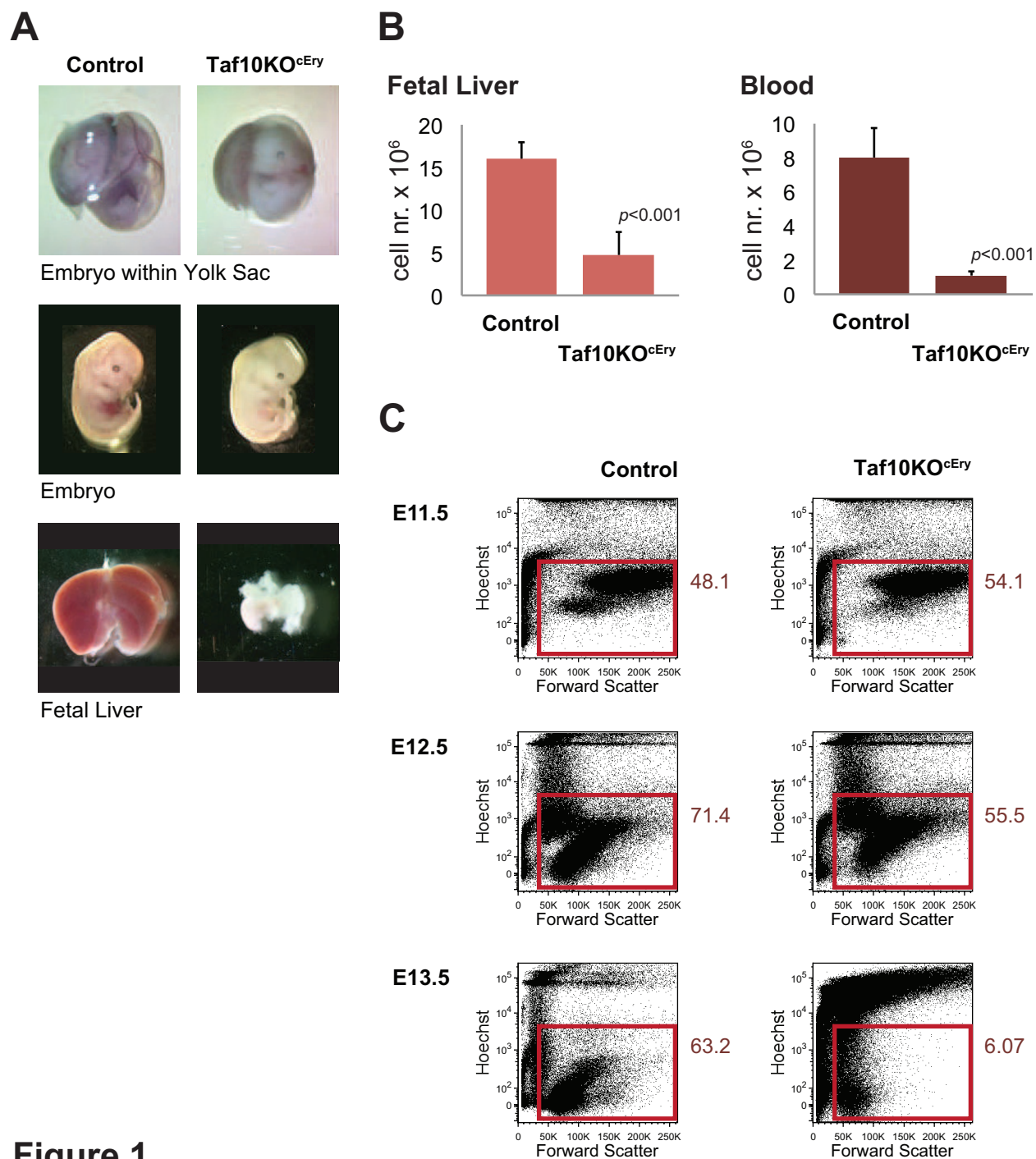


Figure 1

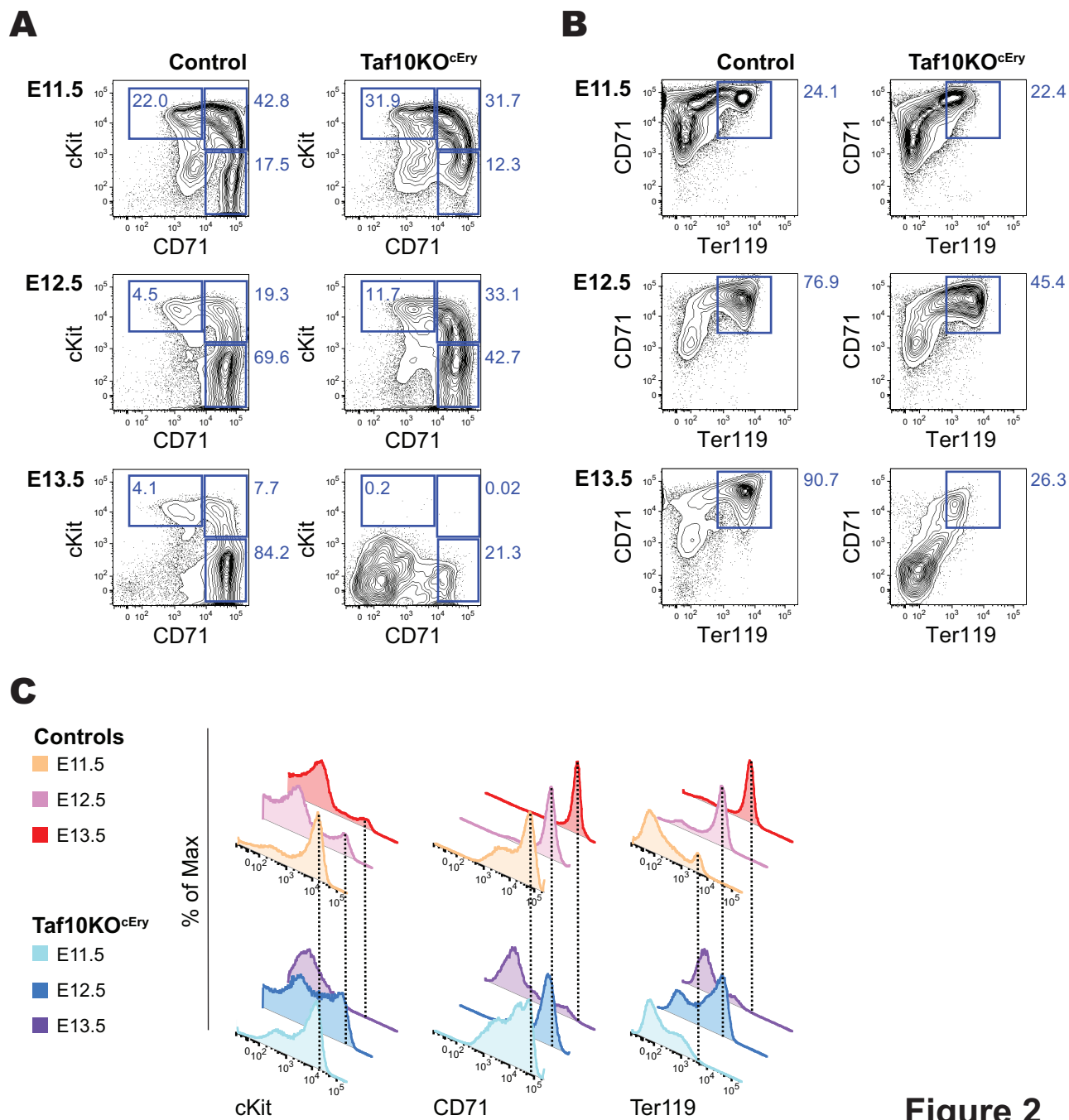
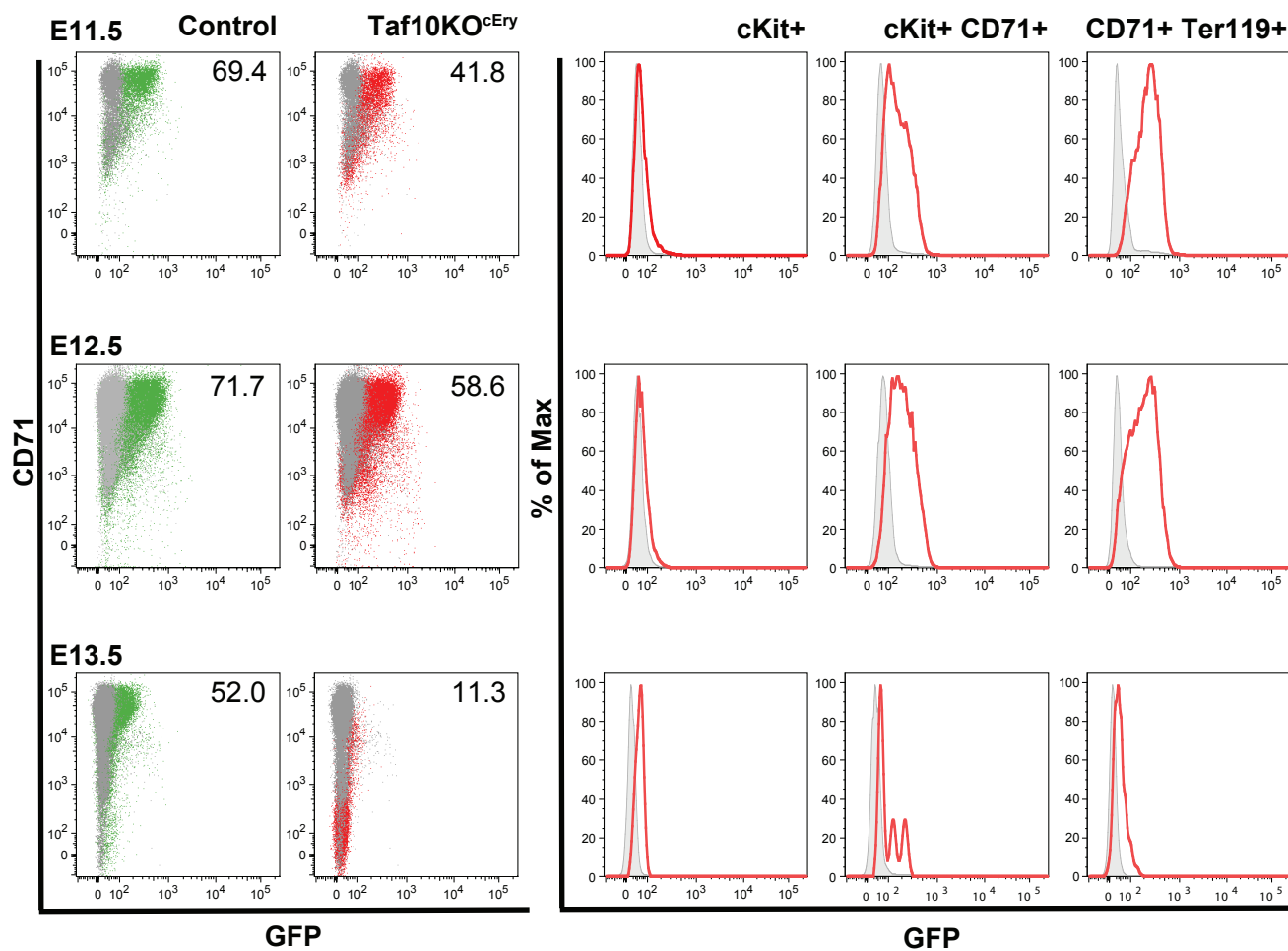


Figure 2

**Figure 3**

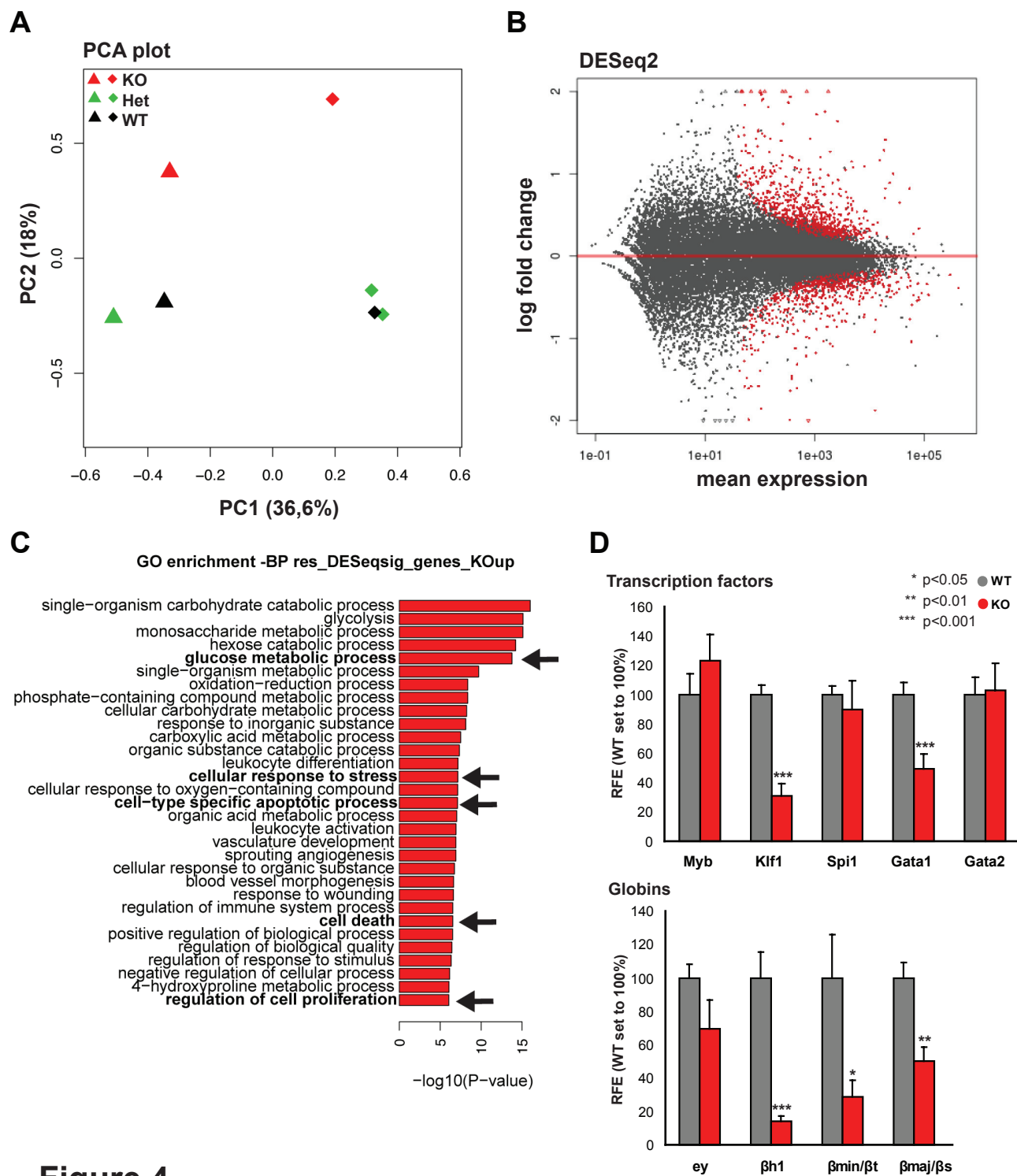


Figure 4

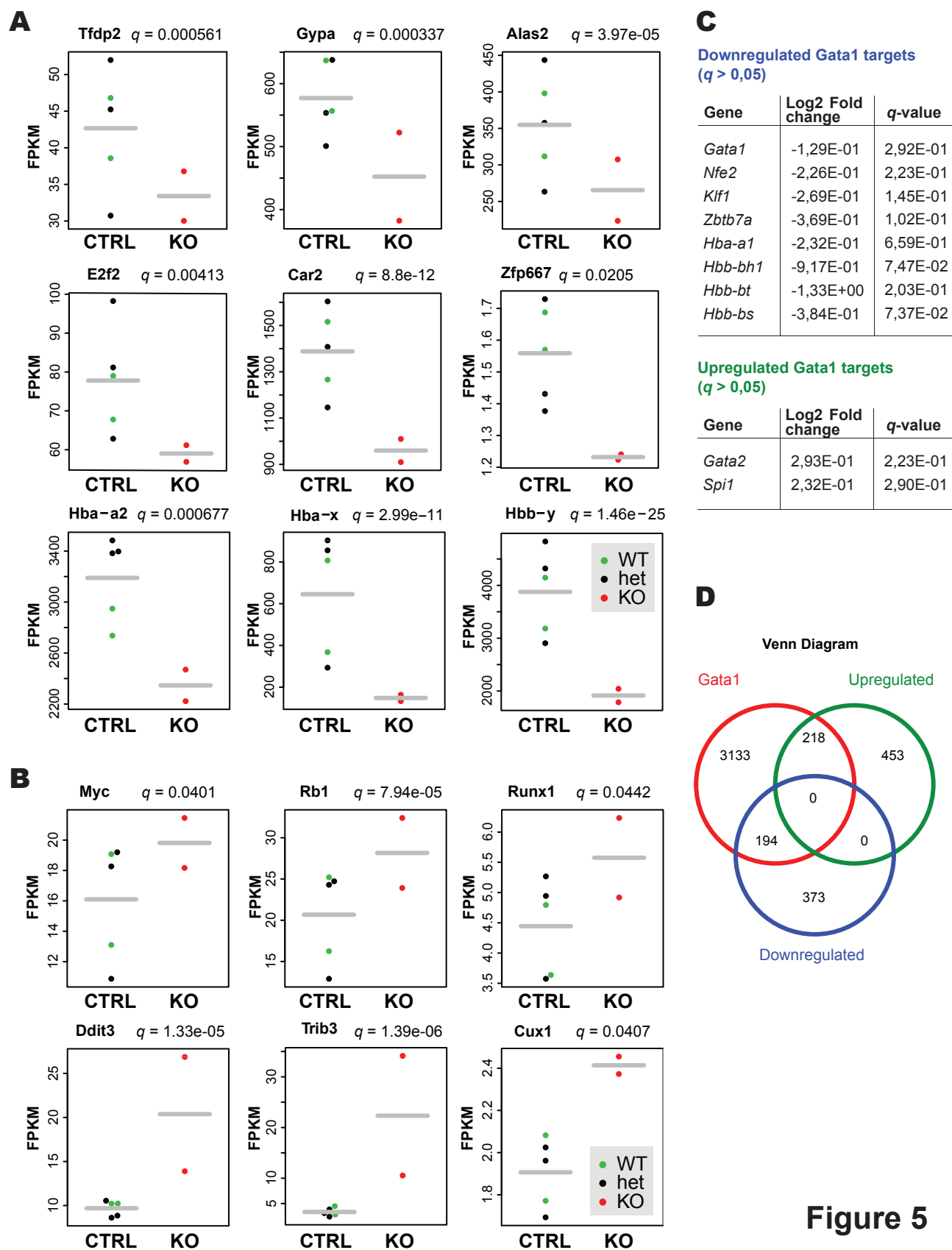
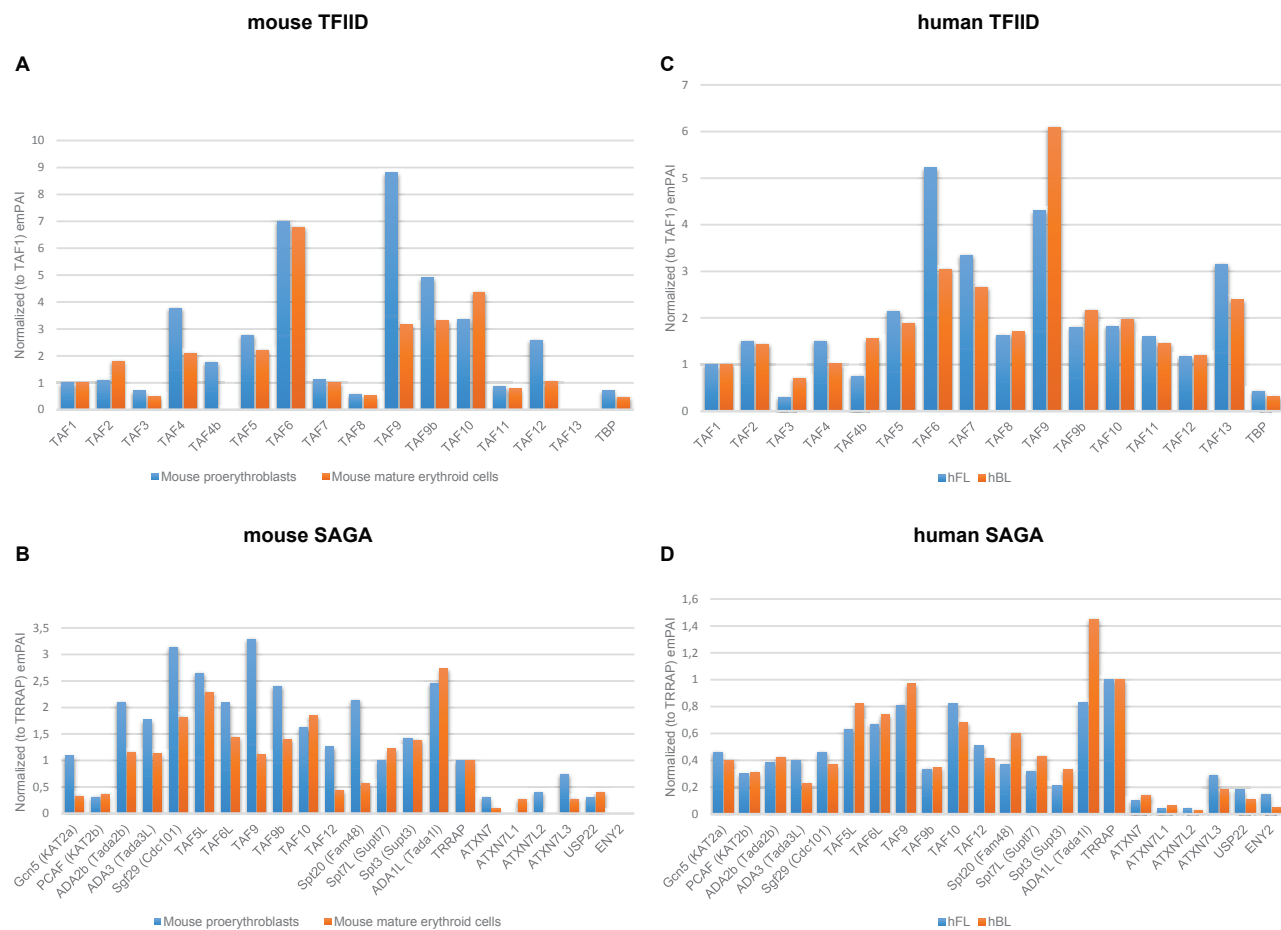


Figure 5

**Figure 6**

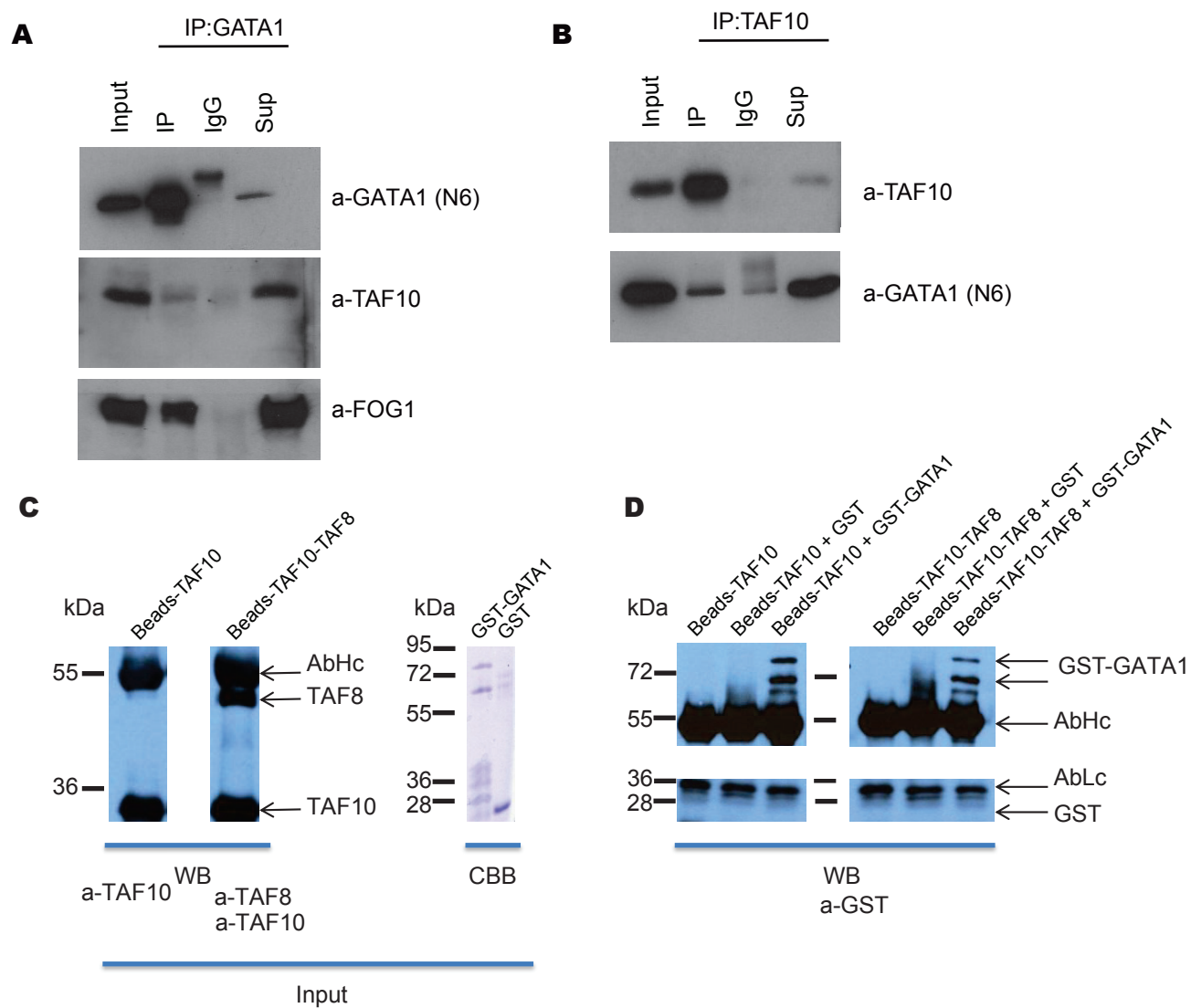
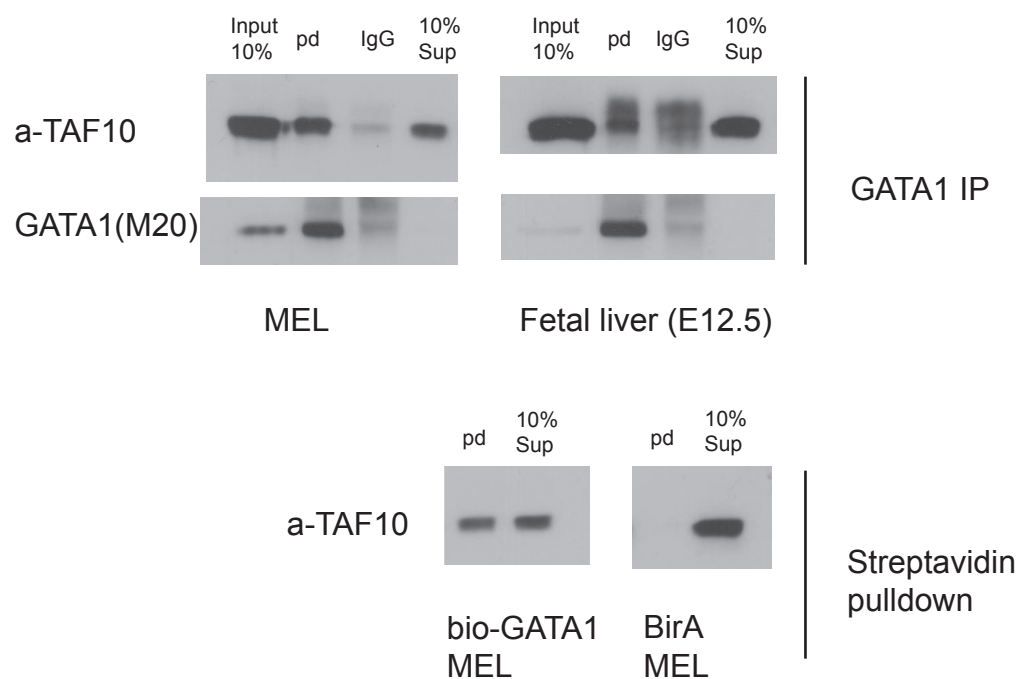


Figure 7

A



B

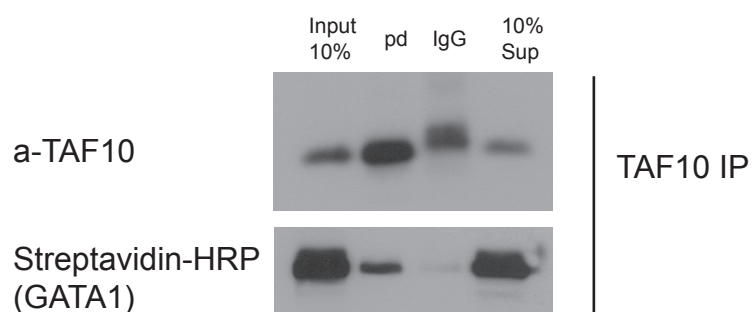
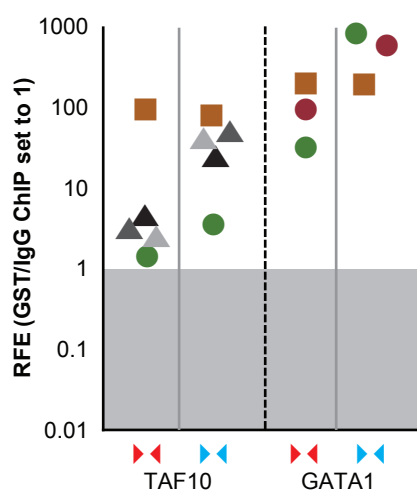


Figure 8

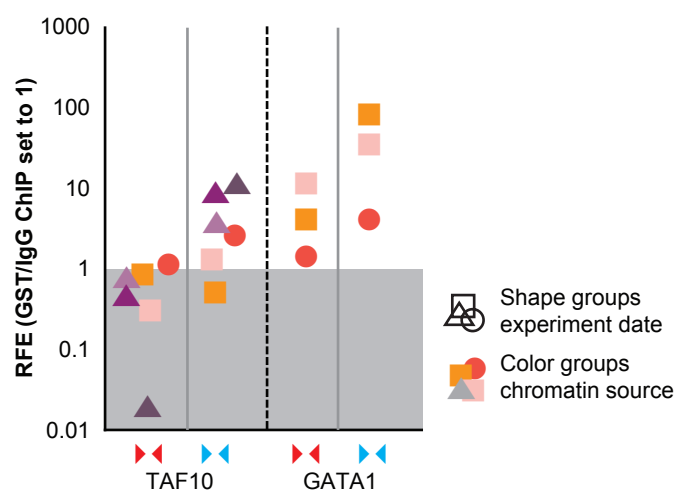
A Human Gata1 promoter



B Fetal Liver ChIP



Adult Blood ChIP



C Compilation ChIP

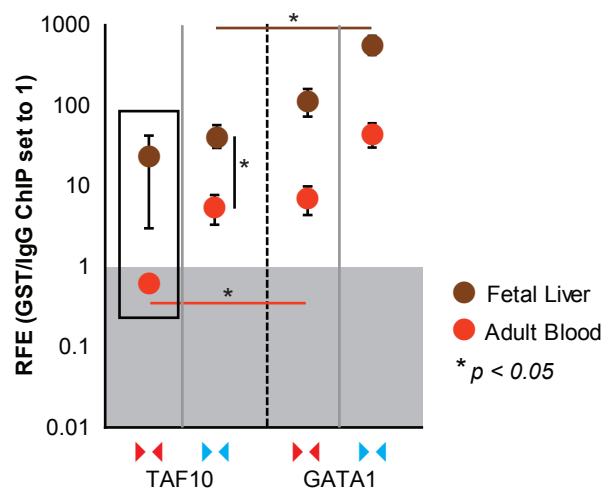


Figure 9

| | Embryonic day | Control | Taf10KO ^{cEry} | p value |
|---------------|---------------|--------------------|-------------------------|---------|
| % Live | E11.5 | 39.55 ± 7.51 | 38.20 ± 22.49 | NS |
| | E12.5 | 63.39 ± 5.94 | 52.53 ± 4.16 | < 0.005 |
| | E13.5 | 60.69 ± 3.21 | 6.55 ± 6.13 | < 0.001 |
| % cKit | E11.5 | 22.45 ± 5.99 | 35.15 ± 4.60 | NS |
| | E12.5 | 5.61 ± 0.98 | 11.47 ± 1.24 | < 0.001 |
| | E13.5 | 3.85 ± 0.43 | 0.35 ± 0.40 | < 0.001 |
| % cKit CD71 | E11.5 | 37.78 ± 6.96 | 20.95 ± 15.20 | NS |
| | E12.5 | 16.30 ± 2.84 | 26.43 ± 5.67 | < 0.05 |
| | E13.5 | 8.03 ± 1.10 | 0.05 ± 0.03 | < 0.001 |
| % CD71 | E11.5 | 17.10 ± 5.85 | 7.79 ± 6.38 | NS |
| | E12.5 | 69.48 ± 3.19 | 50.95 ± 6.16 | < 0.01 |
| | E13.5 | 82.92 ± 2.09 | 14.50 ± 6.85 | < 0.001 |
| % CD71 Ter119 | E11.5 | 29.00 ± 9.29 | 14.95 ± 10.54 | NS |
| | E12.5 | 78.15 ± 1.99 | 55.93 ± 7.21 | < 0.01 |
| | E13.5 | 89.99 ± 1.64 | 14.57 ± 8.79 | < 0.001 |
| cKit MFI | E11.5 | 11121.63 ± 1768.39 | 10149.00 ± 2604.98 | NS |
| | E12.5 | 2645.51 ± 126.30 | 3331.04 ± 618.45 | NS |
| | E13.5 | 1440.50 ± 331.33 | 221.98 ± 188.65 | < 0.001 |
| CD71 MFI | E11.5 | 41095.75 ± 5407.63 | 19293.50 ± 12581.55 | NS |
| | E12.5 | 36305.74 ± 2721.79 | 31207.59 ± 1445.95 | < 0.001 |
| | E13.5 | 43745.10 ± 2266.78 | 3034.50 ± 1274.59 | < 0.001 |
| Ter119 MFI | E11.5 | 1312.75 ± 250.17 | 647.50 ± 7.78 | < 0.001 |
| | E12.5 | 3175.30 ± 215.79 | 2194.38 ± 323.44 | < 0.005 |
| | E13.5 | 3734.50 ± 339.00 | 359.75 ± 92.00 | < 0.001 |

Table 1. Flow cytometry analysis of fetal livers

Statistical analysis derived from the flow cytometry analysis of fetal livers of Taf10KO^{cEry} and control embryos at E11.5, E12.5 and E13.5. At least 3 embryos are analyzed per genotype/stage.

| Protein mouse{m ^{FLcl} }/human{h ^{FL} ,h ^{PB} } /HELA TAF10IP | emPAI | Unique pept |
|--|--|---|
| TAF10 | 5.1/8.68(h ^{FL}),4.29(h ^{PB})/8.68 | 5/5(h ^{FL}),5(h ^{PB})/5 |
| GATA-1 ^{#,§} | 0.08/0.1(h ^{FL}) | 1/1(h ^{FL}) |
| TAL-1 [#] | 0.1(h ^{FL}) | 1(h ^{FL}) |
| LDB-1 [#] | 0.24(h ^{FL}) | 3(h ^{FL}) |
| CNOT1 | 0.54/0.03(h ^{PB}) | 31/2(h ^{PB}) |
| CNOT3 | 0.04 | 1 |
| CNOT9 | 0.34/0.12 | 3/1 |
| CNOT10 | 0.04/0.15(h ^{FL}) | 1/1(h ^{FL}) |
| TRIM28 | 0.35/0.4(h ^{FL}),0.44(h ^{PB})/0.45 | 8/7(h ^{FL}),8(h ^{PB})/9 |
| CBX3 | 2.01/0.88(h ^{FL}) | 5/4(h ^{FL}) |
| CCAR1 [§] | 0.05/0.14(h ^{FL})/0.26 | 2/5(h ^{FL})/9 |
| MED1 [§] | 0.04(h ^{FL})/0.04 | 2(h ^{FL})/3 |

Table 2. Selected activators and cofactors found in the TAF10IP by mass spectromerty (MS)

Human (h^{FL}, h^{PB}) and mouse (m^{FLcl}: fetal liver cell lines) nuclear extracts of erythroid progenitor cells were used. Parameters of MS (emPAI and unique peptides) for each protein in different colors indicating species of origin and cell type are given. Symbols (#: proteins found in the same complex, §: reported to interact with each other).

| <i>TFIID</i> [#] / <i>SAGA</i> [#] | emPAI | Unique Pept |
|--|-------|-------------|
| TAF1 | 0.02 | 4 |
| TAF4a | 0.1 | 2 |
| TAF6 | 0.23 | 5 |
| <i>TAF5L</i> | 0.46 | 8 |
| <i>TAF9</i> [#] | 3.34 | 12 |
| <i>TAF9b</i> [#] | 0.94 | 6 |
| <i>TAF10</i> [#] | 0.17 | 1 |
| TBP | 0.35 | 4 |
| PCAF(KAT2B) | 0.12 | 5 |
| ADA3(TADA3L) | 0.25 | 5 |
| Spt20(Fam48) | 0.06 | 2 |
| Spt3(Supt3) | 0.19 | 3 |

Table 3. Mass spectrometry of GATA1 IP in MEL cells

TFIID and SAGA subunits were identified by MS after GATA1IP (bio-GATA1) on MEL nuclear extracts. Subunits that were found in BirA (Control) cells after streptavidin pulldown were subtracted from the list. Symbols (#): TFIID/SAGA shared subunits